



THE UNIVERSITY *of* EDINBURGH

Edinburgh Research Explorer

Convergent evolution of bacterial ceramide synthesis

Citation for published version:

Stankeviciute, G, Tang, P, Ashley, B, Chamberlain, JD, Hansen, MEB, Coleman, A, D'emilia, R, Fu, L, Mohan, EC, Nguyen, H, Guan, Z, Campopiano, DJ & Klein, EA 2021, 'Convergent evolution of bacterial ceramide synthesis', *Nature Chemical Biology*. <https://doi.org/10.1038/s41589-021-00948-7>

Digital Object Identifier (DOI):

[10.1038/s41589-021-00948-7](https://doi.org/10.1038/s41589-021-00948-7)

Link:

[Link to publication record in Edinburgh Research Explorer](#)

Document Version:

Peer reviewed version

Published In:

Nature Chemical Biology

General rights

Copyright for the publications made accessible via the Edinburgh Research Explorer is retained by the author(s) and / or other copyright owners and it is a condition of accessing these publications that users recognise and abide by the legal requirements associated with these rights.

Take down policy

The University of Edinburgh has made every reasonable effort to ensure that Edinburgh Research Explorer content complies with UK legislation. If you believe that the public display of this file breaches copyright please contact openaccess@ed.ac.uk providing details, and we will remove access to the work immediately and investigate your claim.



1 **Convergent evolution of bacterial ceramide synthesis**

2 Gabriele Stankeviciute^{1,2}, Peijun Tang³, Ben Ashley³, Joshua D. Chamberlain¹, Matthew E.B.
3 Hansen⁴, Aimiya Coleman¹, Rachel D’Emilia¹, Larina Fu¹, Eric C. Mohan³, Hung Nguyen¹,
4 Ziqiang Guan^{5,*}, Dominic J. Campopiano^{3,*}, and Eric A. Klein^{1,2,6,*}.

5
6 **Affiliations:**

7 ¹Center for Computational and Integrative Biology, Rutgers University-Camden, Camden, NJ
8 08102, USA

9 ²Rutgers Center for Lipid Research, Rutgers University, New Brunswick, NJ 08901, USA

10 ³East Chem School of Chemistry, University of Edinburgh, Edinburgh EH9 3FJ, United
11 Kingdom

12 ⁴Department of Genetics, Perelman School of Medicine at the University of Pennsylvania,
13 Philadelphia, PA 19104, USA

14 ⁵Department of Biochemistry, Duke University Medical Center, Durham, NC 27710, USA

15 ⁶Biology Department, Rutgers University-Camden, Camden, NJ 08102, USA.

16 *Correspondence to: eric.a.klein@rutgers.edu, Dominic.Campopiano@ed.ac.uk, and
17 ziqiang.guan@duke.edu

18

19 **Abstract:** The bacterial domain produces numerous types of sphingolipids with various
20 physiological functions. In the human microbiome, commensal and pathogenic bacteria use these
21 lipids to modulate the host inflammatory system. Despite their growing importance, their
22 biosynthetic pathway remains undefined since several key eukaryotic ceramide synthesis
23 enzymes have no bacterial homologue. Here we used genomic and biochemical approaches to
24 identify six proteins comprising the complete pathway for bacterial ceramide synthesis.
25 Bioinformatic analyses revealed the widespread potential for bacterial ceramide synthesis
26 leading to our discovery of the first Gram-positive species to produce ceramides. Biochemical
27 evidence demonstrated that the bacterial pathway operates in a different order than in eukaryotes.
28 Furthermore, phylogenetic analyses support the hypothesis that the bacterial and eukaryotic
29 ceramide pathways evolved independently.

30

31

32 **Introduction**

33 Sphingolipids are found ubiquitously in eukaryotes from fungi, to plants, to animals. By
34 contrast, this class of lipids has been identified in only a handful of bacterial taxa¹. Within this
35 small group of sphingolipid-producing bacteria there is a tremendous variety of acyl chain length
36 and degree of saturation, acyl chain hydroxylation, and lipid headgroups. This structural
37 diversity is paralleled by a wide range of physiological roles for sphingolipids including
38 modulation of host-microbe interactions^{2,3}, protection from bacteriophage⁴, bacterial life cycle
39 and sporulation⁵, and microbial predation⁶. Deeper investigations into the mechanistic roles of
40 sphingolipids in bacterial physiology and host-microbe interactions have been hampered by a
41 lack of knowledge of their biosynthetic pathway. Due to their importance in human health and
42 disease⁷, it is not surprising that the eukaryotic biosynthesis pathway has been elucidated in
43 tremendous detail⁸. By contrast, bacteria do not appear to have homologous enzymes, except for
44 serine palmitoyltransferase (Spt) which performs the initial conserved step in ceramide
45 synthesis^{9,10}.

46 To date, the presence of predicted *spt* genes is the only indication that a bacterial species
47 may synthesize sphingolipids¹¹. However, the presence of a predicted Spt alone is not a
48 particularly reliable indicator of sphingolipid production because there is a high degree of
49 similarity between members of the larger family of α -oxoamine synthases that are involved in
50 heme and biotin synthesis. Here, we identified and characterized the remainder of the bacterial
51 ceramide synthetic pathway. We note that during the preparation of this manuscript, the same set
52 of genes were identified in *C. crescentus*¹². While the independent identification of this
53 biosynthetic pathway corroborates the importance of these genes in ceramide synthesis, our
54 biochemical data suggested a different function for these enzymes than that originally

55 proposed¹². Furthermore, the elucidation of the bacterial ceramide synthesis pathway enabled us
56 to perform a bioinformatic screen that led to the identification of 17 taxonomic classes, including
57 the first Gram-positive bacteria, with the potential to synthesize sphingolipids. Lipid profiling of
58 one of these Actinobacteria provided the first demonstration of Gram-positive bacterial
59 ceramides, validated our bioinformatic approach, and suggested that bacterial sphingolipid
60 synthesis occurs across a wide range of organisms. Surprisingly, the bacterial enzymes are not
61 phylogenetically related to those in eukaryotes and the biosynthetic steps occur in a different
62 order than in eukaryotes. These findings support the independent evolution of ceramide
63 production in bacteria and eukaryotes.

64

65 **Results**

66 Characterization of serine palmitoyltransferase (Spt)

67 The first step in *de novo* ceramide synthesis, which is conserved between eukaryotes and
68 prokaryotes, is the decarboxylative, Claisen-like condensation of palmitoyl-coenzyme A
69 (palmitoyl-CoA) and L-serine into 3-ketosphinganine (3-KDS, **1**) (Fig. 1a)¹³. In *C. crescentus*,
70 we previously identified *ccna_01220* as a putative Spt since the $\Delta ccna_01220$ strain had no
71 detectable ceramide⁴. His-tagged recombinant CCNA_01220 was purified from *E. coli* (see
72 Extended Data Fig. 1a-b); it displayed Spt activity, and the production of 3-KDS was detected by
73 matrix-assisted laser desorption ionization mass spectrometry (MALDI-MS) (Fig. 1b). Kinetic
74 analyses yielded K_m values of $110.40 \pm 13.37 \mu\text{M}$ and $2.98 \pm 0.25 \text{ mM}$ for C16:0-CoA and L-
75 serine, respectively (Fig. 1c), which are comparable to the values determined for *Sphingomonas*
76 *paucimobilis* and human Spt¹⁴⁻¹⁶. *C. crescentus* Spt also condensed serine and C16:1-CoA with
77 similar kinetic parameters (see Extended Data Fig. 1c-d). Liquid chromatography/electrospray

78 ionization-tandem mass spectrometry (LC/ESI-MS/MS) analysis of the ceramide molecule from
79 *C. crescentus* showed that C16:0 was preferentially used as the Spt substrate to form the long-
80 chain base (see Extended Data Fig. 1e). In some organisms, such as the gut commensal
81 *Bacteroides thetaiotaomicron*, 1-deoxysphingolipids can be detected when Spt uses alanine as a
82 substrate rather than serine². Similarly, a *C. crescentus* serine auxotroph ($\Delta serA$), produced 1-
83 deoxyceramide (see Extended Data Fig. 1f-g).

84

85 Genetic screen identifies the ceramide synthesis pathway

86 In the absence of ceramides, *C. crescentus* becomes resistant to the cationic antimicrobial
87 peptide, polymyxin B (PMX) and increasingly sensitive to bacteriophage $\Phi cr30$ ⁴. Using these
88 two phenotypes of ceramide depletion, we performed a transposon mutagenesis screen
89 incorporating both positive and negative selection to identify candidate genes involved in
90 ceramide synthesis (see Extended Data Fig. 2A, detailed in Materials and Methods). Transposon
91 insertions in cells displaying both selection phenotypes were mapped (see Supplementary Data
92 Table 1 and Extended Data Fig. 2b) and multiple insertions were found in the *spt* gene validating
93 this approach. These transposon mutants served as a platform for identifying ceramide synthesis
94 enzymes as described below.

95 Spt enzymes vary in their preferred acyl-CoA substrate; some enzymes utilize fatty acyl-
96 CoA thioesters whereas others use an acyl-chain bound as a thioester to an acyl carrier protein
97 (ACP). Our genetic screening identified *ccna_01223*, a putative acyl-CoA synthetase, which
98 adds CoA to a long-chain fatty acid. Additionally, inspection of neighboring genes revealed a
99 candidate ACP (*ccna_01221*). This genomic arrangement of the Spt, ACP, and ACP-synthetase
100 is similar to that seen in *Sphingomonas wittichii*¹⁷. Although no transposon insertions were

101 identified in *ccna_01221*, this was not surprising given that the gene is only 261 bp and would
102 therefore have a low probability of containing an insertion. Deletion of either gene resulted in a
103 total loss of ceramides (see Extended Data Fig. 3a-b) and both deletions could be complemented
104 by ectopic expression of the respective gene (see Extended Data Fig. 3a-b). Total ion and
105 extracted ion chromatograms confirm that the deletions did not disrupt global lipid production
106 (see Extended Data Fig. 3c-d and Supplementary Table 3).

107 In eukaryotes, the second synthetic step is the reduction of 3-KDS to sphinganine (**2**),
108 which is catalyzed by a NADPH-dependent 3-ketodihydrosphinganine reductase (KDSR) (Fig.
109 1a). Among our transposon insertions, *ccna_01222* was annotated as an NADH ubiquinone-
110 oxidoreductase. Deletion of *ccna_01222* resulted in a ceramide molecule with a mass reduction
111 of 2 Da (Fig. 2a), corresponding to a loss of two hydrogens. Tandem mass spectrometry
112 (MS/MS) analysis confirmed the retention of the oxidized double bond on the 3-KDS derived
113 sphingoid base (see Extended Data Fig. 4). Complementation of the *ccna_01222* deletion
114 restored ceramide reduction (Fig. 2a). These data suggest that the bacterial reductase acts after
115 the second acyl chain is added to 3-KDS. This contrasts with the eukaryotic pathway where
116 deletion of KDSR generally leads to an accumulation of 3-KDS substrate and prevents
117 downstream reactions¹⁸. There have been reports of 3-KDS being acylated directly by ceramide
118 synthase in eukaryotic cells; however, this was only observed when Spt was highly
119 overexpressed and cells were provided with excess serine and palmitate¹⁹. Since the bacterial
120 reductase uses oxidized ceramide (oxCer) (**6**) as a substrate, we have named CCNA_01222
121 Ceramide Reductase (CerR).

122 In eukaryotes, the second acyl chain is attached to the sphingoid backbone by ceramide
123 synthase (CerS) to form dihydroceramide (**4**) (Fig. 1a). Analysis of our transposon hits pointed to

124 *ccna_01212* as a potential CerS. In *C. crescentus*, this gene is annotated as a dATP
125 pyrophosphohydrolase; however, closely related genes identified by BLAST have a variety of
126 annotations including Gcn5-related N-acetyltransferase (GNAT). Deletion of *ccna_01212* led to
127 a complete loss of ceramides (Fig. 2b), consistent with its role in ceramide synthesis. To confirm
128 the enzymatic activity of CCNA_01212, recombinant protein purified from *E. coli* (see Extended
129 Data Fig. 5a-b) was incubated with the substrates 3-KDS and palmitoyl-CoA. LC/ESI-MS/MS
130 analysis of the reaction product identified the expected ceramide molecule (Fig. 2c). Kinetic
131 analyses showed that CCNA_01212 constitutively hydrolyzed acyl-CoA even in the absence of
132 3-KDS, and the reaction exhibits substrate inhibition (see Extended Data Fig. 5c). Upon the
133 addition of 3-KDS, the reaction proceeded according to Michaelis-Menten kinetics and we
134 determined the $K_{m,app}$ for C16:0-CoA to be $21.3 \pm 4.1 \mu\text{M}$ (see Extended Data Fig. 5c). Based on
135 these data we have named CCNA_01212 bacterial Ceramide Synthase (bCerS). Since eukaryotic
136 CerS enzymes have specific acyl-chain specificities²⁰, we assessed the substrate preference of *C.*
137 *crescentus* bCerS. Recombinant bCerS was incubated with 3-KDS and an equimolar mixture of
138 acyl-CoA substrates ranging from C8-C24, and the relative amount of the respective products
139 was monitored by LC/ESI-MS. *C. crescentus* had the highest *in vitro* activity with C14 and
140 showed very little activity with acyl-CoA thioesters of 18 carbons or longer (see Extended Data
141 Fig. 5d). *In vivo*, the C16 ceramide product is most abundant rather than C14 (see Extended Data
142 Fig. 1e); this may reflect the fact that C16 accounts for 30% of the fatty acid content of the cell,
143 whereas C14 is only 2%²¹. Our experiments demonstrating bCerS activity with acyl-CoA as a
144 substrate are consistent with ceramide synthase activity; however, given that the acyl-CoA is
145 readily hydrolyzed by bCerS to a free fatty acid, we cannot rule out the possibility that bCerS
146 ligates the fatty acid to 3-KDS via a reverse-ceramidase-like mechanism²².

147 A common ceramide modification found in fungi, plants, some animal tissues, and
148 bacteria is the addition of a hydroxyl group to form phytoceramides (**4**) (Fig. 1a). In plants,
149 sphingoid base hydroxylase 1/2 (Sbh1/2) adds a hydroxyl group to sphinganine to form
150 phytosphingosine (**3**) prior to the addition of the second acyl chain²³. In mammals, DES2 has
151 dual Δ^4 -desaturase and C-4 hydroxylase activities enabling the hydroxylation of ceramide (**5**) to
152 phytoceramide²⁴. *C. crescentus* does not have a homologue of Sbh1/2; DES2 has some
153 homology to the fatty acid desaturase CCNA_03535, though deletion of *ccna_03535* did not
154 abolish ceramide hydroxylation. We did not identify any putative hydroxylases in our transposon
155 screen; however, we hypothesized that this modification may not have a strong effect on one or
156 both of our selection phenotypes. To focus on genes that promoted PMX-resistance only, we
157 searched the Fitness Browser database²⁵ and found that the disruption of *ccna_00202*, a DesA-
158 family fatty acid desaturase/hydroxylase, results in PMX resistance. Deletion of *ccna_00202* led
159 to a ceramide molecule with a mass reduction of 16 Da corresponding to the loss of a hydroxyl
160 group (Fig. 2d). Complementation of *ccna_00202* restored ceramide hydroxylation (Fig. 2d).
161 Tandem MS/MS data are consistent with the hydroxylation occurring on C2 of the acyl chain
162 (see Extended Data Fig. 4). For this reason, we have named CCNA_00202 Ceramide
163 Hydroxylase (CerH). Examination of the mass spectra of the CerR deletion mutant showed that
164 hydroxylation remains in the absence of reduction (Fig. 2a). Mechanistically, this suggests that
165 CerH can use either DHC or oxCer as a substrate, or that acyl chain hydroxylation occurs
166 upstream of oxCer reduction.

167 The ceramide in *C. crescentus* has a monounsaturated acyl chain (see Extended Data Fig.
168 1e). Acyl chain desaturation has also been reported in *Sphingomonas* species²⁶. Attempts to
169 identify a desaturase were unsuccessful. *C. crescentus* encodes at least four DesA-family

170 desaturases (*ccna_00203*, *ccna_01515*, *ccna_01743*, and *ccna_03535*). Deletion of each of these
171 genes individually or in combination had no effect on ceramides. While there could be other, yet
172 unidentified, desaturases, we hypothesized that *C. crescentus* bCerS may have a preference for
173 monounsaturated acyl-CoA substrates. *In vitro*, recombinant bCerS had a 3-fold greater
174 preference for C16:1-CoA over C16:0-CoA as a substrate (see Extended Data Fig. 5e); the
175 saturated and monounsaturated C16 fatty acids are present in equal amounts *in vivo*²¹. *C.*
176 *crescentus* encodes two orthologues each of FabA/FabB which are involved in the synthesis of
177 monounsaturated fatty acids²⁷. These four genes are all essential²⁸ which precluded direct tests of
178 our hypothesis. Since many bacteria produce fully saturated ceramides^{2,5}, it appears that this
179 modification is not a universal feature of bacterial ceramide synthesis.

180 The observations of oxCer in the Δ *cerR* strain (Fig. 2a) and the ability of bCerS to use 3-
181 KDS as a substrate (Fig. 2c) suggested that the order of the synthetic pathway in bacteria is
182 different than that in eukaryotes. Based on the MS data, we can propose the following model for
183 bacterial ceramide synthesis (Fig. 2e). Spt condenses serine with an acyl-thioester (either acyl-
184 ACP or acyl-CoA) to produce 3-KDS. bCerS uses 3-KDS and a second palmitoyl-CoA to
185 generate oxCer which is subsequently reduced to ceramide by CerR. We considered the
186 possibility that CerR may work upstream of bCerS, as in eukaryotes. In this case, an alternative
187 model is that bCerS can use either 3-KDS or sphinganine as a substrate leading to oxCer or
188 ceramide as the final product, respectively. *In vitro* assays using recombinant bCerS show that
189 the enzyme can use either substrate (Fig. 2c and Extended Data Fig. 5f). To determine which
190 pathway was more likely to occur *in vivo*, we used fluorescently-tagged proteins to infer the
191 subcellular localization of the synthetic enzymes. Incubation of bacteria with chloroform-
192 saturated Tris buffer results in the preferential permeabilization of the outer membrane and

193 leakage of soluble periplasmic proteins²⁹ (Fig. 2f). Using this approach with the three core
194 ceramide synthesis genes showed that Spt and bCerS retained fluorescence while the CerR signal
195 was entirely lost (Fig. 2f). Consistent with the purification of recombinant Spt and bCerS as
196 soluble proteins, these imaging studies suggest that Spt and bCerS are cytoplasmic whereas CerR
197 is a soluble periplasmic protein. Though we cannot rule out other mechanisms, the spatial
198 separation of these proteins *in vivo* is consistent with our model in which bCerS acts upstream of
199 CerR (Fig. 2e).

200 Bacterial ceramides can be modified in a variety of species-specific manners including
201 fatty acid hydroxylation (Fig. 2d), acyl chain branching², and head group modification by
202 phosphorylation² or glycosylation⁴. In *C. crescentus*, we previously identified two sphingolipid
203 glycosyltransferases⁴ and here we report the discovery of a ceramide hydroxylase CerH (Fig.
204 2d).

205

206 Bioinformatic identification of ceramide producing species

207 The identification of Spt, bCerS, and CerR as the core bacterial ceramide synthetic
208 enzymes in *C. crescentus* presented the opportunity to find orthologues in other species and
209 perform a bioinformatic screen for additional potential ceramide producers. Sphingolipids have
210 been isolated from the oral pathogen *Porphyromonas gingivalis*³. The *spt* gene (*pgn_1721*) has
211 been identified³ and BLAST analysis of bCerS and CerR suggested that PGN_0374 and
212 PGN_1886 are the respective orthologues despite having limited homology (PGN_0374: 25%
213 identical, 43% similar; PGN_1886: 23% identical, 43% similar). Additionally, unlike in *C.*
214 *crescentus*, the proposed *P. gingivalis* genes are not in the same genomic locus. To test their
215 functionality, we complemented *C. crescentus* deletion strains with the corresponding *P.*

216 *gingivalis* genes. Complementation with *spt* (*pgn_1721*)³⁰ yielded both the expected *C.*
217 *crenscentus* ceramide (m/z 588.465 Da) as well as a ceramide with two additional methylene units
218 (m/z 614.478 Da) (Fig. 3a). These data are consistent with previous studies showing that *P.*
219 *gingivalis* has a substrate preference for 17, 18, and 19-carbon fatty-acyl-CoA substrates³¹.

220 Complementation of $\Delta bcerS$ with *pgn_0374* restored ceramide synthesis (Fig. 3b); a
221 variety of ceramide molecules were observed suggesting that, like Spt, the *P. gingivalis* bCerS
222 has different substrate preferences than the *C. crescentus* orthologue. Lastly, *P. gingivalis* *cerR*
223 (*pgn_1886*) was able to rescue ceramide reduction (Fig. 3c). Together, these results demonstrate
224 that screening for organisms with this set of genes could yield a broader set of bacteria with the
225 potential to synthesize ceramides.

226 A BLAST analysis of Spt, bCerS and CerR against the NCBI prokaryotic representative
227 genomes database (5,700+ representative bacterial organisms; see Materials and Methods and
228 Supplementary Data 1 for detailed search parameters and E-value cutoffs) identified 272
229 organisms, belonging to 17 taxonomic classes, containing orthologues of all three genes (Fig. 3d,
230 Supplementary Data 1, and Extended Data Fig. 6). Analysis of the distance between these core
231 genes showed that, in most clades, the genes were within 10 kb of one another (see Extended
232 Data Fig. 7a). However, among the Bacteroides these genes were found scattered throughout the
233 genome (see Extended Data Fig. 7a); this is consistent with the high degree of chromosomal
234 plasticity and genomic rearrangements associated with these organisms³². Whereas all previously
235 identified ceramide producers are Gram-negative organisms, our bioinformatic analysis
236 suggested that several Gram-positive Actinobacteria may be competent for ceramide synthesis.
237 Lipidomic analyses confirmed the presence of dihydroceramide in *Streptomyces aurantiacus*,
238 providing the first evidence of ceramide lipids in Gram-positive bacteria (Fig. 3e). MS/MS

239 analysis of *S. aurantiacus* showed that, in contrast to *C. crescentus*, fatty acid desaturation
240 occurred on the long-chain base (LCB) (see Extended Data Fig. 7b). Based on phylogenetic
241 clustering of the individual ceramide synthesis genes (Extended Data Fig. 6), as well as the fact
242 that the three genes are found in a putative operon, it is possible that the ceramide synthesis
243 cassette may have been acquired in these Actinobacteria by horizontal gene transfer from
244 Deltaproteobacteria.

245 In eukaryotes, organisms often have multiple CerS isoforms with distinct fatty acyl-CoA
246 specificities. For example, the six human CerS isoforms enable the synthesis of ceramides with
247 acyl chain lengths of 14-26 carbons²⁰. We performed a bioinformatic search to identify bacterial
248 species with multiple bCerS isoforms and found 22 candidates among the Alphaproteobacteria,
249 Bacteroidia, Balneolia, Chitinophagia, and Rhodothermia (see Supplementary Data 2). In most
250 cases, the two bCerS homologues were far apart on the chromosome making it impossible to
251 know whether the two proteins were truly bCerS isoforms or simply similar N-acetyltransferases.
252 One exception was *Prevotella buccae*, where the two candidate *bcerS* genes were encoded
253 immediately next to one another (HMPREF0649_00885 and HMPREF0649_00886; 57%
254 identical and 74% similar). We complemented the *C. crescentus* $\Delta bcerS$ strain with each of the
255 *P. buccae* isoforms and found that while both could rescue ceramide synthesis, each enzyme
256 produced distinct lipid products (Fig. 3f). HMPREF0649_00885 preferred a fully saturated LCB
257 substrate while HMPREF0649_00886 used a desaturated LCB (see Extended Data Fig. 7c-d).

258

259 *Independent evolution of ceramide production in bacteria*

260 While the Spt enzyme catalytic residues are conserved between eukaryotic and bacterial
261 species (see Extended Data Fig. 8), neither CerR nor bCerS share obvious homology to KDSR or

262 CerS, respectively. The closest eukaryotic homologue to CerR is NADH dehydrogenase 1A
263 subcomplex subunit 9 (NDUF9A), which is a component of Complex I in the mitochondrial
264 oxidative phosphorylation pathway. Conversely, the bacterial relatives of KDSR are annotated as
265 short-chain dehydrogenases³³. While both reductase families have conserved catalytic and NAD-
266 binding sites³⁴ (see Extended Data Fig. 9), human KDSR and *C. crescentus* CerR are only 27%
267 similar and 14% identical. Phylogenetic clustering of these proteins showed that CerR evolved
268 its ceramide reductase activity convergently, arising from NDUF9A-related genes (Fig. 4a).

269 Similarly, bCerS is a member of the GNAT family of acyltransferases. Bacteria have a
270 variety of GNAT proteins which are closely related to eukaryotic Gcn5 acyltransferases.
271 Phylogenetic analysis demonstrated that bCerS is a subgroup of bacterial GNATs whereas the
272 eukaryotic CerS is only distantly related to Gcn5 family proteins (Fig. 4b). Indeed, eukaryotic
273 CerS has a highly conserved Lag1P domain^{35,36} which is not found in any of the bCerS proteins
274 (see Extended Data Fig. 10). These phylogenetic analyses, coupled with the proposed reordering
275 of the synthetic pathway (Fig. 1a and 2f-g), demonstrate that ceramide synthesis evolved
276 independently in bacteria and eukaryotes.

277

278 **Discussion**

279 Since the discovery of sphingolipids in the late 19th century by Johann L.W. Thudichum,
280 thousands of publications have demonstrated these lipids to be ubiquitous throughout Eukarya; to
281 date, there are over 500 published headgroup variants and acyl chain modifications among this
282 lipid group (LIPID MAPS,³⁷). The diversity of sphingolipids reflects the multifunctional roles of
283 these molecules: the sphingoid backbone provides structural integrity to the cell membrane, the

284 headgroups are involved in lipid-mediated interactions, and some sphingolipid-derivatives
285 function as intracellular second messengers⁷.

286 The list of bacterial sphingolipid-producing species is comparatively short but growing.
287 Their presence in several taxa begs the question of ‘how widespread could this lipid be?’. Our
288 results identify the key enzymes required for bacterial ceramide synthesis. While the Spt enzyme
289 is homologous between prokaryotes and eukaryotes, bCerS and CerR are unique to bacteria. We
290 note a recent publication also identified these genes as being involved in ceramide synthesis in *C.*
291 *crescentus*¹². The authors proposed, without direct evidence, that these proteins carry out the
292 same functions as their eukaryotic counterparts (see Reference ¹², Figure 11). However, our
293 biochemical analyses demonstrate that CerR and bCerS have unique enzymatic activities and the
294 sequence of synthetic reactions in the bacterial pathway is likely different than that in eukaryotes
295 (Fig. 1a and 2f). The previous findings regarding bacterial ceramide synthesis are actually
296 consistent with our proposed pathway; their thin-layer chromatography (TLC) analysis of the
297 CerR deletion yielded an unidentified band which is likely oxCer (see Reference ¹², Figure 9,
298 $\Delta 1164$, top-most band). Additionally, ectopic expression of Spt and CerR in *E. coli* did not yield
299 sphinganine, while expression of Spt and bCerS did lead to the production of the fast migrating
300 sphingolipid species (see Reference ¹², Figure S4). As this molecule does not occur in
301 eukaryotes, they lacked a TLC standard to confirm the identity of this band leading to a
302 challenge in interpreting the data.

303 Though our data support a mechanism in which bCerS directly adds an acyl chain to 3-
304 KDS, we note that the metabolic intermediate sphinganine has been detected in *B.*
305 *thetaitotaomicron*². We have tried several lipid extraction methods as well as stable-isotope
306 labeling but have never detected sphinganine in *C. crescentus*. While it is possible that the

307 ceramide synthesis pathway operates differently in *Bacteroides*, given the conservation of this
308 enzyme as well as the ability of the *P. gingivalis* enzyme to complement the deletion in *C.*
309 *crenscentus* that seems less likely. An alternative hypothesis is that *Bacteroides* has a ceramidase
310 enzyme, which is lacking in *C. crescentus*, that hydrolyzes ceramide to sphinganine. Indeed, a
311 bioinformatic search identified two linear amide CN-hydrolases (pfam PF02275; of which
312 ceramidases are members) in *B. thetaiotaomicron*. One of these enzymes hydrolyzes bile acids,
313 however, the function of the second homologue is unknown³⁸. *C. crescentus* does not have a
314 homologue of these proteins. Additionally, *B. thetaiotaomicron* can assimilate and metabolize
315 sphinganine from the host gut to produce ceramide lipids³⁹. Not surprisingly, the details of SL
316 biosynthesis vary in different bacteria and a working hypothesis is that that their environmental
317 niches provide an opportunity for the utilization of particular SL metabolic pathways. Further
318 characterization of the structures and mechanisms of these enzymes will be necessary to elucidate
319 their physiological functions.

320 Coupled with phylogenetic analysis, our data support a model in which bacterial
321 ceramide synthesis evolved convergently and independently of the eukaryotic pathway. This type
322 of evolution, where identical substrates and products are metabolized by distinct enzymes, is
323 well characterized particularly in plants. For example, 1) gibberellins (tetracyclic diterpenoid
324 carboxylic acids) are produced by unique enzymes in plants and fungi⁴⁰, 2) several independent
325 enzymatic pathways are used to produce caffeine among plant species⁴¹, and 3) the UDP-
326 glucosyltransferases and β -glucosidases used in the synthesis of benzoxazinoids evolved
327 independently in different plant lineages⁴². One potential mechanism for the independent
328 evolution of metabolic pathways is gene duplication and modification of substrate specificity. In
329 the case of bacterial ceramide synthesis, the CerR protein in *C. crescentus* is related to the
330 NDUF9A-domain protein CCNA_03718 (27% identical and 46% similar). In this study, we

331 found that *P. buccae* encodes two bCerS proteins (57% identical and 74% similar) with unique
332 substrate preferences (Fig. 3f).

333 Phylogenetic analysis of the three ceramide synthetic genes has identified a wide range of
334 Gram-negative, as well as several Gram-positive, species with the potential to produce
335 ceramides. These organisms occupy a range of habitats including aquatic, soil, and within animal
336 hosts. Among the small subset of previously identified ceramide-producing species, these lipids
337 play roles in outer membrane integrity⁴³, defense against bacteriophage⁴, protection against
338 extracellular stress¹², suppression of host inflammation², and their production can be
339 developmentally regulated⁵. Furthermore, lipidomic analyses of these organisms has identified a
340 wide range of ceramide species with varying acyl chain length and saturation, acyl chain
341 hydroxylation, and head group glycosylation and phosphorylation; the consequences of these
342 modifications are yet to be determined. By defining the microbial blueprint for ceramide
343 synthesis, we now have a platform for dissecting the physiological functions of these lipids and
344 for potentially engineering the production of novel sphingolipids.

345
346 **Acknowledgments:** The authors thank Carla Cugini (Rutgers University) for providing *P.*
347 *gingivalis* genomic DNA for cloning. The authors also thank Anthony Geneva (Rutgers
348 University-Camden) for helpful discussions. Funding was provided by National Science
349 Foundation grants MCB-1553004 and MCB-2031948 (E.A.K.), National Institutes of Health
350 grants GM069338 and R01AI148366 (Z.G.), and Biotechnology and Biological Sciences
351 Research Council grants BB/M010996/1 and BB/T016841/1 (D.J.C.).

352

353 **Author contributions:** G.S. made the mutant and complementation strains for characterizing the
354 synthetic pathway and performed the lipid extractions. P.T., B.A., and E.C.M. purified and
355 characterized the recombinant proteins. J.D.C. cloned and analyzed the *P. buccae*
356 complementation strains. M.E.B.H. and E.A.K. performed the phylogenetic and bioinformatic
357 analyses. E.A.K. acquired the microscopy images. A.C., R.D., L.F., and H.N. performed the
358 transposon screen to isolate ceramide deficient mutants. Z.G. performed the lipid mass
359 spectrometry analyses. G.S., P.T., B.A., Z.G., D.J.C., and E.A.K. designed the experiments,
360 interpreted the data, and wrote the manuscript.

361

362 **Competing interests:** Authors declare no competing interests.

363

364 **Figure Legends**

365

366 **Figure 1. CCNA_01220 is a functional serine palmitoyltransferase (Spt).** (a) The schematic
367 depicts the eukaryotic ceramide synthesis pathway. In some organisms, phytoceramides (**4**) are
368 produced by adding a hydroxyl group (OH) to the sphingoid base (**3**) (Sph) or to ceramide (**5**)
369 (DES2). (b) Recombinant Spt was incubated with the indicated substrates for 1 hr and reaction
370 products were analyzed by MALDI-MS. The final panel shows a theoretical mass spectrum for
371 the expected product, 3-KDS. (c) Kinetic analyses of Spt determined the Km for L-serine (upper)
372 and C16:0-CoA (lower) (n=3; data are presented as mean +/- SD).

373

374 **Figure 2. A genetic screen identified ceramide synthesis enzymes.** (a-d) Negative ion ESI/MS
375 shows the $[M + Cl]^-$ ions of the lipids emerging at 2 to 3 min. Ceramide species are labelled with

376 a red dot and the modified lipid moiety is designated with a red-dashed oval. Note that MS/MS
377 analysis of ceramide from *C. crescentus* shows that the desaturation occurs on the acyl chain (see
378 Extended Data Fig. 1e); however, we have not determined the precise position of the double
379 bond. In this, and all subsequent figures, the structural cartoons only indicate which acyl chain is
380 desaturated, but not the exact position of the double bond. Relative quantification of all the major
381 lipid species for each mass spectrum is available in Supplementary Table 3. (a) Lipids were
382 extracted from wild-type, $\Delta ccna_01222$, and *ccna_01222*-complemented cells. (b) Lipids were
383 extracted from $\Delta ccna_01212$ and *ccna_01212*-complemented cells. (c) Recombinant
384 CCNA_01212 was incubated with 40 μ M 3-KDS and 50 μ M C16:0-CoA for 1 hr and the
385 reaction product was analyzed by normal phase LC/ESI-MS in negative ion mode. (d) Lipids
386 were extracted from $\Delta ccna_00202$ and *ccna_00202*-complemented cells. (e) Based on the MS
387 data above, we proposed the following model for bacterial ceramide synthesis. The genes
388 comprising this synthetic pathway are in close proximity in the genome (see Extended Data Fig.
389 2b). (f) Cells expressing the indicated fluorescently-tagged proteins were grown overnight in the
390 presence of inducer. GspG-mCherry and TAT-mCherry are control inner-membrane and
391 periplasmic proteins, respectively. Control and permeabilized cells were imaged by fluorescence
392 microscopy to monitor the loss of fluorescence upon permeabilization. The results are the
393 overlay of phase and fluorescent images. Scale bar = 5 μ m.

394

395 **Figure 3. Bioinformatic analysis identifies a wide range of potential ceramide-producing**
396 **bacteria.** (a-c) Deletions of the *spt* (a), *bcerS* (b), and *cerR* (c) genes in *C. crescentus* were
397 complemented with the indicated homologues from *P. gingivalis*. Lipids extracted from these
398 strains were analyzed by normal phase LC/ESI-MS in negative ion mode. $[M + Cl]^-$ ions of the

399 ceramide species emerging at 2 to 3 min are shown with ceramide species labelled with a red dot.
400 (d) Bacterial species with homologues to all three ceramide synthesis enzymes are clustered by
401 the overall homology of the 3 proteins (see Methods). Bootstrap percentage values are indicated
402 by shaded circles at each node. Branches are colored by taxonomic class and Gram-positive
403 Actinobacteria are labeled. (e) Negative ion ESI/MS shows the $[M + Cl]^-$ ions of the ceramide
404 species (emerging at 2 to 3 min) extracted from *S. aurantiacus*. Ceramide is labelled with a red
405 dot. Determination of the ceramide structure by MS/MS is provided in Extended Data Fig. 7b. (f)
406 Deletion of *bcerS* in *C. crescentus* was complemented by two *bcerS* orthologues from *P. buccae*.
407 $[M + Cl]^-$ ions of the ceramide species emerging at 2 to 3 min are shown with ceramide species
408 labelled with a red dot. Determination of the ceramide structures by MS/MS is provided in
409 Extended Data Figs. 7c-d.

410
411 **Figure 4. Phylogenetic analysis indicates convergent evolution of ceramide synthesis.** (a-b)
412 Unrooted trees built using the maximum likelihood method show the distance between
413 eukaryotic and bacterial ceramide synthesis genes as well as their closest homologues. Bootstrap
414 percentage values are indicated by shaded circles at each node. (a) Bacterial CerR is most closely
415 related to eukaryotic and bacterial proteins of the NDUF9A family, a subunit of mitochondrial
416 Complex I. By contrast, Eukaryotic KDSR is homologous to bacterial short-chain
417 dehydrogenases, unrelated to CerR. (b) Bacterial bCerS is part of a larger family of GNAT
418 acyltransferases, which are, in turn closely related to eukaryotic Gcn5 proteins. By contrast,
419 eukaryotic CerS proteins are distant from the Gcn5-related proteins.

420

421

422 **Data availability:**

423 The raw data for Figure 1C and Extended Data Figures 1c-d, 5c-e, and 7a are provided as
424 Microsoft Excel files in the supplementary information (Source Data 1-4). The data for the
425 bioinformatic analyses was obtained from the following publicly available NCBI resources:
426 NCBI Prokaryotic Representative Genomes:
427 https://ftp.ncbi.nlm.nih.gov/genomes/GENOME_REPORTS/prok_representative_genomes.txt.
428 Accession numbers for the proteins used for BLAST analyses are as follows. Bacterial Spt
429 homologues: *C. crescentus* YP_002516593.1; *P. gingivalis* BAG34240; *M. xanthus* ABF87747;
430 *B. stolpii* BAF73753. Bacterial bCerS homologues: *C. crescentus* YP_002516585.1; *P.*
431 *gingivalis* BAG32893; *M. xanthus* ABF92629; *B. stolpii* WP_102243213. Bacterial CerR
432 homologues: *C. crescentus* YP_002516595.1; *P. gingivalis* BAG34405; *M. xanthus* ABF87537;
433 *B. stolpii* WP_102243212. Eukaryotic CerS homologues: Human P27544.1; *A. thaliana*
434 NP_001184985; *S. cerevisiae* AAA21579.1. Eukaryotic Spt homologues: Human NP_006406.1;
435 *A. thaliana* NP_190447.1; *S. cerevisiae* CAA56805.1. Eukaryotic KDSR homologues: Human
436 NP_002026.1; *A. thaliana* NP_187257; *S. cerevisiae* P38342. Eukaryotic Gcn5 homologues:
437 Human AAC39769.1 and *S. cerevisiae* NP_011768.1.
438

439 **References**

440

441 1 Harrison, P. J., Dunn, T. M. & Campopiano, D. J. Sphingolipid biosynthesis in man and
442 microbes. *Nat Prod Rep* **35**, 921-954 (2018).

443 2 Brown, E. M. *et al.* Bacteroides-derived sphingolipids are critical for maintaining
444 intestinal homeostasis and symbiosis. *Cell Host Microbe* **25**, 668-680 e667 (2019).

445 3 Moye, Z. D., Valiuskyte, K., Dewhirst, F. E., Nichols, F. C. & Davey, M. E. Synthesis of
446 sphingolipids impacts survival of *Porphyromonas gingivalis* and the presentation of
447 surface polysaccharides. *Front Microbiol* **7**, 1919 (2016).

448 4 Stankeviciute, G., Guan, Z., Goldfine, H. & Klein, E. A. *Caulobacter crescentus* adapts
449 to phosphate starvation by synthesizing anionic glyco-glycerolipids and a novel
450 glycosphingolipid. *mBio* **10**, e00107-00119 (2019).

451 5 Ahrendt, T., Wolff, H. & Bode, H. B. Neutral and phospholipids of the *Myxococcus*
452 *xanthus* lipodome during fruiting body formation and germination. *Appl Environ*
453 *Microbiol* **81**, 6538-6547 (2015).

454 6 Kaneshiro, E. S., Hunt, S. M. & Watanabe, Y. Bacteriovorax stolpii proliferation and
455 predation without sphingophosphonolipids. *Biochem Biophys Res Commun* **367**, 21-25
456 (2008).

457 7 Hannun, Y. A. & Obeid, L. M. Sphingolipids and their metabolism in physiology and
458 disease. *Nat Rev Mol Cell Biol* **19**, 175-191 (2018).

459 8 Merrill, A. H., Jr. Sphingolipid and glycosphingolipid metabolic pathways in the era of
460 sphingolipidomics. *Chem Rev* **111**, 6387-6422 (2011).

461 9 Ikushiro, H., Hayashi, H. & Kagamiyama, H. A water-soluble homodimeric serine
462 palmitoyltransferase from *Sphingomonas paucimobilis* EY2395T strain. Purification,
463 characterization, cloning, and overproduction. *J Biol Chem* **276**, 18249-18256 (2001).

464 10 Yard, B. A. *et al.* The structure of serine palmitoyltransferase; gateway to sphingolipid
465 biosynthesis. *J Mol Biol* **370**, 870-886 (2007).

466 11 Geiger, O., Gonzalez-Silva, N., Lopez-Lara, I. M. & Sohlenkamp, C. Amino acid-
467 containing membrane lipids in bacteria. *Prog Lipid Res* **49**, 46-60 (2010).

468 12 Olea-Ozuna, R. J. *et al.* Five structural genes required for ceramide synthesis in
469 *Caulobacter* and for bacterial survival. *Environ Microbiol* (2020).

470 13 Wadsworth, J. M. *et al.* The chemical basis of serine palmitoyltransferase inhibition by
471 myriocin. *J Am Chem Soc* **135**, 14276-14285 (2013).

472 14 Harrison, P. J. *et al.* Use of isotopically labeled substrates reveals kinetic differences
473 between human and bacterial serine palmitoyltransferase. *J Lipid Res* **60**, 953-962 (2019).

474 15 Li, S., Xie, T., Liu, P., Wang, L. & Gong, X. Structural insights into the assembly and
475 substrate selectivity of human SPT-ORMDL3 complex. *Nat Struct Mol Biol* **28**, 249-257
476 (2021).

477 16 Raman, M. C. *et al.* The external aldimine form of serine palmitoyltransferase: structural,
478 kinetic, and spectroscopic analysis of the wild-type enzyme and HSN1 mutant mimics.
479 *J Biol Chem* **284**, 17328-17339 (2009).

480 17 Raman, M. C., Johnson, K. A., Clarke, D. J., Naismith, J. H. & Campopiano, D. J. The
481 serine palmitoyltransferase from *Sphingomonas wittichii* RW1: An interesting link to an
482 unusual acyl carrier protein. *Biopolymers* **93**, 811-822 (2010).

- 483 18 Ren, J. *et al.* Quantification of 3-ketodihydrosphingosine using HPLC-ESI-MS/MS to
484 study SPT activity in yeast *Saccharomyces cerevisiae*. *J Lipid Res* **59**, 162-170 (2018).
- 485 19 Zheng, W. *et al.* Ceramides and other bioactive sphingolipid backbones in health and
486 disease: lipidomic analysis, metabolism and roles in membrane structure, dynamics,
487 signaling and autophagy. *Biochim Biophys Acta* **1758**, 1864-1884 (2006).
- 488 20 Tidhar, R. *et al.* Eleven residues determine the acyl chain specificity of ceramide
489 synthases. *J Biol Chem* **293**, 9912-9921 (2018).
- 490 21 Chow, T. C. & Schmidt, J. M. Fatty acid composition of *Caulobacter crescentus*.
491 *Microbiology* **83**, 369-373 (1974).
- 492 22 Okino, N. *et al.* The reverse activity of human acid ceramidase. *J Biol Chem* **278**, 29948-
493 29953 (2003).
- 494 23 Chen, M., Markham, J. E., Dietrich, C. R., Jaworski, J. G. & Cahoon, E. B. Sphingolipid
495 long-chain base hydroxylation is important for growth and regulation of sphingolipid
496 content and composition in *Arabidopsis*. *Plant Cell* **20**, 1862-1878 (2008).
- 497 24 Omae, F. *et al.* DES2 protein is responsible for phytoceramide biosynthesis in the mouse
498 small intestine. *Biochem J* **379**, 687-695 (2004).
- 499 25 Price, M. N. *et al.* Mutant phenotypes for thousands of bacterial genes of unknown
500 function. *Nature* **557**, 503-509 (2018).
- 501 26 Kawahara, K., Moll, H., Knirel, Y. A., Seydel, U. & Zähringer, U. Structural analysis of
502 two glycosphingolipids from the lipopolysaccharide-lacking bacterium *Sphingomonas*
503 *capsulata*. *European Journal of Biochemistry* **267**, 1837-1846 (2000).

504 27 Feng, Y. & Cronan, J. E. *Escherichia coli* unsaturated fatty acid synthesis: complex
505 transcription of the *fabA* gene and in vivo identification of the essential reaction catalyzed
506 by FabB. *J Biol Chem* **284**, 29526-29535 (2009).

507 28 Christen, B. *et al.* The essential genome of a bacterium. *Mol Syst Biol* **7**, 1-7 (2011).

508 29 Stankeviciute, G. *et al.* Differential modes of crosslinking establish spatially distinct
509 regions of peptidoglycan in *Caulobacter crescentus*. *Mol Microbiol* **111**, 995-1008
510 (2019).

511 30 Rocha, F. G. *et al.* *Porphyromonas gingivalis* sphingolipid synthesis limits the host
512 inflammatory response. *J Dent Res* **99**, 568-576 (2020).

513 31 Mun, J. *et al.* Structural confirmation of the dihydrosphinganine and fatty acid
514 constituents of the dental pathogen *Porphyromonas gingivalis*. *Org Biomol Chem* **5**,
515 3826-3833 (2007).

516 32 Nguyen, M. & Vedantam, G. Mobile genetic elements in the genus *Bacteroides*, and their
517 mechanism(s) of dissemination. *Mob Genet Elements* **1**, 187-196 (2011).

518 33 Kavanagh, K. L., Jornvall, H., Persson, B. & Oppermann, U. Medium- and short-chain
519 dehydrogenase/reductase gene and protein families : the SDR superfamily: functional and
520 structural diversity within a family of metabolic and regulatory enzymes. *Cell Mol Life*
521 *Sci* **65**, 3895-3906 (2008).

522 34 Boyden, L. M. *et al.* Mutations in KDSR cause Recessive Progressive Symmetric
523 Erythrokeratoderma. *Am J Hum Genet* **100**, 978-984 (2017).

524 35 Kageyama-Yahara, N. & Riezman, H. Transmembrane topology of ceramide synthase in
525 yeast. *Biochem J* **398**, 585-593 (2006).

526 36 Spassieva, S. *et al.* Necessary role for the Lag1p motif in (dihydro)ceramide synthase
527 activity. *J Biol Chem* **281**, 33931-33938 (2006).

528 37 Liebisch, G. *et al.* Update on LIPID MAPS classification, nomenclature and shorthand
529 notation for MS-derived lipid structures. *J Lipid Res* (2020).

530 38 Yao, L. *et al.* A selective gut bacterial bile salt hydrolase alters host metabolism. *Elife* **7**
531 (2018).

532 39 Lee, M. T., Le, H. H. & Johnson, E. L. Dietary sphinganine is selectively assimilated by
533 members of the mammalian gut microbiome. *J Lipid Res* **62**, 100034 (2021).

534 40 Tudzynski, B. Gibberellin biosynthesis in fungi: genes, enzymes, evolution, and impact
535 on biotechnology. *Appl Microbiol Biotechnol* **66**, 597-611 (2005).

536 41 Huang, R., O'Donnell, A. J., Barboline, J. J. & Barkman, T. J. Convergent evolution of
537 caffeine in plants by co-option of exapted ancestral enzymes. *Proc Natl Acad Sci U S A*
538 **113**, 10613-10618 (2016).

539 42 Dick, R. *et al.* Comparative analysis of benzoxazinoid biosynthesis in monocots and
540 dicots: independent recruitment of stabilization and activation functions. *Plant Cell* **24**,
541 915-928 (2012).

542 43 Kawasaki, S. *et al.* The cell envelope structure of the lipopolysaccharide-lacking gram-
543 negative bacterium *Sphingomonas paucimobilis*. *J Bacteriol* **176**, 284-290 (1994).

544 44 Madeira, F. *et al.* The EMBL-EBI search and sequence analysis tools APIs in 2019.
545 *Nucleic Acids Res* (2019).

546 45 Lowther, J. *et al.* Role of a conserved arginine residue during catalysis in serine
547 palmitoyltransferase. *FEBS Lett* **585**, 1729-1734 (2011).

548

549 **Materials and Methods**

550

551 **Bacterial strains, plasmids, and growth conditions**

552 The strains, plasmids, and primers used in this study are described in Supplementary Tables 4, 5,
553 and 6, respectively. Strain construction details are available in a Supplementary Note. *C.*

554 *crenscentus* wild-type strain NA1000 and its derivatives were grown at 30 °C in peptone-yeast-
555 extract (PYE) medium for routine culturing. To control serine concentration for the serine

556 auxotrophic strain, *C. crescentus* was grown in Hutner-Imidazole-Glucose-Glutamate (HIGG)

557 media⁴⁶ with variable amounts of serine (0-10 mM). *E. coli* strains were grown at 37 °C in LB

558 medium. When necessary, antibiotics were added at the following concentrations: kanamycin 30

559 µg/ml in broth and 50 µg/ml in agar (abbreviated 30:50) for *E. coli* and 5:25 for *C. crescentus*;

560 tetracycline 12:12 *E. coli* and 1:2 *C. crescentus*; spectinomycin 50:50 *E. coli* and 25:100 *C.*

561 *crescentus*; and ampicillin 50:100 *E. coli*. Gene expression was induced in *C. crescentus* with

562 either 0.3% (w/v) xylose or 0.5 mM vanillate. *Streptomyces aurantiacus* was grown in

563 International Streptomyces Project Synthetic Salts-Starch Medium (ISP4) at 30 °C.

564

565 **Genetic screen for ceramide synthesis enzymes**

566 A conjugation-competent and diaminopimelic acid (DAP) auxotrophic strain of *E. coli*

567 (MFDpir,⁴⁷) carrying the kanamycin-encoding mini-Tn5 plasmid pBAM1 (Addgene #60487,⁴⁸)

568 was grown overnight in LB media containing 0.3 mM DAP. Wild-type *C. crescentus* was grown

569 overnight in PYE. In a microcentrifuge tube, 1 ml of *C. crescentus* was mixed with 100 µl of *E.*

570 *coli*, the cells were washed once in PYE, and the final cell pellet was resuspended in 20 µl PYE.

571 The concentrated cell sample was dropped onto a PYE agar plate containing 0.3 mM DAP and

572 incubated at 30 °C for 6 hr. After incubation, the cells were scraped into 1 ml of PYE, vortexed,
573 and spread onto PYE agar plates containing 25 µg/ml kanamycin and 200 µg/ml polymyxin B. In
574 the absence of DAP, the donor *E. coli* strain could not grow, the kanamycin selected for
575 transposon insertions, and the polymyxin B selected for potentially ceramide-deficient cells.
576 Colonies were picked into duplicate 96-well plates containing 200 µl PYE per well +/- 2 µl
577 bacteriophage φCr30. Each plate had one well of wild-type control and one well with no cells, as
578 a control for contamination. Approximately 20 sets of duplicate plates were inoculated. Plates
579 were incubated overnight at 30 °C and growth was measured in a BMG Labtech CLARIOstar
580 plate reader by absorbance at 660 nm. The 94 phage-containing wells that had the lowest OD₆₆₀
581 were considered potential hits. The corresponding wells from the non-infected plates were
582 consolidated into new 96-well plates and treated +/- phage as above. Growth curves were
583 acquired for 27 hr on a BMG Labtech CLARIOstar plate reader incubating at 30 °C with
584 shaking. The ratio of the final to the maximal OD₆₆₀ for each well was calculated and normalized
585 to the wild-type control. Wells with a ratio less than that of the wild-type control were kept for
586 further characterization. To determine the site of transposon insertion we used arbitrarily-primed
587 PCR with primer pairs EKS153/S159 and EKS154/S160 as previously described⁴⁸.

588

589 **Cloning and purification of *C. crescentus* Spt**

590 The *ccna_01220* gene was amplified with primers EK1107/1108. A C-terminal 6-histidine tag
591 expression vector (pET-28a, EMD Biosciences) was amplified with primers EK1131/1106 and
592 the insert was ligated using HiFi Assembly (New England Biolabs). The resulting plasmid was
593 transformed into *E. coli* BL21 (DE3) cells. One colony was grown overnight in Terrific Broth
594 (TB)/kanamycin at 37 °C with shaking. The inoculant was diluted into TB/kanamycin to OD₆₀₀

595 of 0.1. When the OD₆₀₀ reached 0.8, protein expression was induced with 0.5 mM isopropyl-β-
596 D-1-thiogalactopyranoside (IPTG), and cultures were grown at 16 °C overnight. Cells were
597 harvested by centrifugation at 5,000 x g for 7 min. The cell pellets were resuspended in 20 mM
598 potassium phosphate buffer, pH 7.5, 250 mM NaCl, 30 mM imidazole and 25 μM pyridoxal
599 phosphate (PLP). The cells were sonicated on ice (Soniprep 150, 10 cycles of 30 seconds on/30
600 seconds off), cell lysates were cleared by centrifugation at 24,000 x g for 40 min, and
601 supernatants were filtered through a 0.45 μm filter. The recombinant Spt was purified using an
602 Äkta FPLC system (Cytiva) and a HisTrap HP 1 ml Ni²⁺ column (Cytiva) with an imidazole
603 gradient from 30 mM to 500 mM, followed by size exclusion chromatography (SEC) on a
604 HiLoad 16/600 Superdex 200 preparatory grade column (Cytiva) with a buffer containing 20
605 mM potassium phosphate, pH 7.5, 250 mM NaCl, 10% (v/v) glycerol and 25 μM PLP. The
606 purification was monitored by SDS-PAGE and Coomassie blue staining.

607

608 **Cloning and purification of *C. crescentus* bCerS**

609 The *ccna_01212* gene was amplified with primers EK1199/1269 and cloned into the
610 NdeI/HindIII site of plasmid pET-28a to generate an N-terminal 6-histidine tag. The construct
611 was transformed into *E. coli* BL21 (DE3) competent cells. One colony was grown overnight in
612 LB broth/kanamycin at 37 °C with shaking. The inoculant was diluted into LB/kanamycin to
613 OD₆₀₀ of 0.1. When the OD₆₀₀ reached 0.8, protein expression was induced with 1 mM IPTG,
614 and cultures were grown at 16 °C overnight. Cells were harvested by centrifugation at 5,000 x g
615 for 7 min. The cell pellets were resuspended in 50 mM Tris-HCl, pH 8.0, 250 mM NaCl, and 30
616 mM imidazole. The cells were sonicated on ice (Soniprep 150, 10 cycles of 30 seconds on/30
617 seconds off), cell lysates were cleared by centrifugation at 24,000 x g for 40 min, and

618 supernatants were filtered through a 0.45 μm filter. The recombinant bCerS was purified using
619 an Äkta FPLC system (Cytiva) and a HisTrap HP 1 ml Ni^{2+} column (Cytiva) with an imidazole
620 gradient from 10 mM to 500 mM, followed by size exclusion chromatography (SEC) on a
621 HiLoad 16/600 Superdex 200 preparatory grade column (Cytiva) with a buffer containing 50
622 mM Tris-HCl, pH 8.0, 250 mM NaCl, and 10% (v/v) glycerol. The purification was monitored
623 by SDS-PAGE and Coomassie blue staining.

624

625 **Mass Spectrometry of recombinant proteins**

626 Purified Spt and bCerS were analyzed in positive ion mode using a liquid chromatography
627 system connected to a Waters Synapt G2 QTOF with an electrospray ionization (ESI) source. 10
628 μL of 10 μM protein was injected into a Phenomenex C4 3.6 μm column. The conditions for the
629 qTOF were source temperature 120 $^{\circ}\text{C}$, backing pressure 2 mbar, and sampling cone voltage
630 54V. The protein was eluted with a 12-minute gradient, starting at 5% acetonitrile with 0.1%
631 formic acid to 95% acetonitrile. The resulting spectra were analyzed using MassLynx V4.1
632 software (Waters Corporation)

633

634 **Determination of kinetic constants for *C. crescentus* Spt**

635 Spt kinetic parameters were determined using a 5,5'-dithiobis-(2-nitrobenzoic acid) (DTNB)
636 assay as previously described¹⁶. The enzyme kinetic assay was carried out in a 96 well microtiter
637 plate containing 0.4 mM DTNB, 1 μM Spt enzyme, 20 mM L-serine, 1-1000 μM C16:0/1-CoA
638 for K_m -C16:0/1-CoA determination or 0.4 mM DTNB, 1 μM Spt enzyme, 0.1-100 mM L-serine,
639 250 μM C16:0/1-CoA for K_m -L-Ser determination in a buffer containing 100 mM HEPES, 250
640 mM NaCl, pH 7.0. The experiments were monitored in a BioTek Synergy HT plate reader at 412

641 nm in 1 min intervals for 60 minutes at 30 °C. The enzyme kinetic constants were calculated by
642 fitting the Michaelis-Menten equation to a plot of reaction rate versus concentration using Origin
643 2019 (OriginLab).

644

645 **Assessing sphingolipid products using MALDI-TOF-MS**

646 Spt reaction products were desalted using OMIX C4 pipette tips (Agilent) and eluted in 100%
647 acetonitrile (ACN) containing 0.2% formic acid. 1 μ L of first matrix seed (20 mg/ml alpha-
648 cyano-4-hydroxycinnamic acid (CHCA) in methanol/acetone (2:3, v/v) was spotted onto a MTP
649 384 ground steel plate (Bruker) and left to air dry. The samples were mixed with the second
650 matrix (20 mg/ml CHCA in 50% ACN within 0.25% trifluoroacetic acid (TFA)) in a 1:1 ratio,
651 and 1 μ L of the mixture was spotted on top of the CHCA-acetone layer and left to air-dry. The
652 samples were analyzed in reflector mode using a calibrated Bruker UltrafleXtreme MALDI-
653 TOF-mass spectrometer. The analysis was carried out in positive ion mode. The laser power was
654 adjusted to provide optimum signal. Each sample was tested with 500 laser shots and each
655 spectrum was a sum of over 5000 shots. Spectra were acquired over a range of m/z 200-1500.
656 The data acquisition software used was Flex Control version 3.4. The data was analyzed using
657 Data Analysis version 4.4 software.

658

659 **Enzymatic activity assay for *C. crescentus* bCerS**

660 The reactions were carried out with 2 μ M bCerS, 40 μ M 3-ketodihydrosphingosine (3-KDS)
661 (dissolved in 0.1% v/v ethanol) and 50 μ M C16-CoA for at least 1 hour in a buffer containing 20
662 mM HEPES, 25 mM KCl, 2 mM MgCl₂, pH 7.5. The reaction products were extracted using the
663 Bligh-Dyer method⁴⁷ and characterized by LC/MS as described below. To assay bCerS substrate

664 specificity, the reaction was carried out as above using equimolar amounts of C8-C24-CoA (total
665 acyl-CoA concentration remained 50 μ M).

666

667 **Determination of kinetic constants for *C. crescentus* bCerS**

668 bCerS kinetic parameters were determined using a DTNB assay as previously described above
669 for Spt. The enzyme kinetic assay was carried out in a 96 well microtiter plate containing 1 mM
670 DTNB, 1.2 mg/ml bCerS enzyme, 0 or 40 μ M 3-KDS, and 1-500 μ M C16:0-CoA for K_m -C16:0-
671 CoA determination in a buffer containing 100 mM HEPES, 150 mM NaCl, pH 7.5. The
672 experiments were monitored in a BioTek Synergy HT plate reader at 412 nm in 30 second
673 intervals for 60 minutes at 30 °C. The enzyme kinetic constants were calculated by fitting the
674 Michaelis-Menten equation to a plot of reaction rate versus concentration using Origin 2019
675 (OriginLab).

676

677 **Lipid extraction**

678 *C. crescentus* strains were grown overnight (5 ml) and lipids were extracted by the method of
679 Bligh and Dyer⁴⁹. Cells were harvested in glass tubes at 10,000 x g for 30 min and the
680 supernatant was removed. The cells were resuspended in 1 ml of water, 3.75 volumes of 1:2
681 (v/v) chloroform: methanol was added, and the samples were mixed by vortexing. Chloroform
682 (1.25 volumes) and water (1.25 volumes) were added sequentially with vortexing to create a two-
683 phase system and the samples were centrifuged at 200 x g for 5 minutes at room temperature.
684 The bottom, organic phase was transferred to a clean tube with a Pasteur pipette and washed
685 twice in “authentic” upper phase. Subsequently, the residual organic phase with the lipids was
686 collected and dried under argon.

687

688 **Lipid analysis by normal phase LC/ESI–MS/MS**

689 Methods for lipid analysis by normal phase LC/ESI–MS/MS have been described⁵⁰. Briefly,
690 normal phase LC was performed on an Agilent 1200 Quaternary LC system equipped with an
691 Ascentis Silica HPLC column, 5 μm , 25 cm \times 2.1 mm (Sigma-Aldrich, St. Louis, MO) as
692 described. The LC eluent (with a total flow rate of 300 $\mu\text{l}/\text{min}$) was introduced into the ESI
693 source of a high resolution TripleTOF5600 mass spectrometer (Applied Biosystems, Foster City,
694 CA). Instrumental settings for negative ion ESI and MS/MS analysis of lipid species were as
695 follows: ion spray voltage (IS) = -4500 V ; curtain gas (CUR) = 20 psi; ion source gas 1 (GSI) =
696 20 psi; declustering potential (DP) = -55 V ; and focusing potential (FP) = -150 V . The MS/MS
697 analysis used nitrogen as the collision gas. Data analysis was performed using Analyst TF1.5
698 software (Applied Biosystems, Foster City, CA). A list of the identified lipid species can be
699 found in Supplementary Table 2. A representative total ion chromatogram (TIC) and its
700 corresponding extracted ion chromatogram (EIC) is available in Extended Data Figs. 3c-d. The
701 peak areas of the EICs of major lipid species are compiled in Supplementary Table 3.

702

703 **Cell permeabilization and labeling**

704 Chloroform-saturated Tris buffer was prepared by mixing 50 mM Tris, pH 7.4 with chloroform
705 (70:30) and shaking the mixture at room temperature for 30 min. Cells to be permeabilized were
706 collected via centrifugation (2 min at 6,000 $\times g$, 4 $^{\circ}\text{C}$) and resuspended in an equal volume of the
707 aqueous phase of the chloroform-saturated Tris buffer. Resuspended cells were rocked for 45
708 min at room temperature and then washed twice in 50 mM Tris, pH 7.4 (via centrifugation for 10

709 min at 5,000 x g) to remove residual chloroform. Control cells were treated as above, but
710 incubated in 50 mM Tris, pH 7.4 without chloroform.

711

712 **Fluorescence microscopy**

713 Cells harboring fluorescent fusions were induced overnight with 0.3% xylose and permeabilized
714 as described above. The permeabilized cells were spotted onto 1% agarose pads. Fluorescence
715 microscopy was performed on a Nikon Ti-E inverted microscope equipped with a Prior Lumen
716 220PRO illumination system, CFI Plan Apochromat 100X oil immersion objective (NA 1.45,
717 WD 0.13 mm), Zyla sCMOS 5.5-megapixel camera (Andor), and NIS Elements v, 4.20.01 for
718 image acquisition.

719

720 **Phylogenetic analysis of bacterial ceramide synthesis genes**

721 Following our identification of Spt, bCerS, and CerR as key enzymes in ceramide synthesis in *C.*
722 *crescentus*, we used BLASTP to find the closest protein homologues in the known ceramide
723 producers *P. gingivalis*, *M. xanthus*, and *B. stolpii* (see Supplementary Data 1). Using each of
724 these proteins as a query, we used TBLASTN to find related proteins in the NCBI prokaryotic
725 representative genomes database (5,700+ representative bacterial organisms). E-value cutoffs
726 were determined by performing a traditional BLASTP with each protein and getting the
727 approximate E-value cutoff for the top 250 hits (see Supplementary Data 1). TBLASTN settings
728 were chosen to only take the top hit for each organism, and we collected the organism name,
729 taxonomic ID, sequence start and end position, strand orientation, and protein sequence.

730 Following the TBLASTN searches, the data were combined and filtered to remove duplicates.

731 We identified organisms that contained hits for all three target genes. To facilitate comparison of

732 these organisms, we made *in silico* fusions by concatenating the Spt, CerR, and bCerS protein
733 sequences. These fused sequences were aligned using MUSCLE aligner⁵¹. Phylogenetic trees
734 were prepared using RAxML (Randomized Axelerated Maximum Likelihood version 8.2.12)⁵²
735 with 100 bootstraps and a maximum-likelihood search. RAxML was run on the CIPRES Portal
736 at the San Diego Supercomputer Center⁵³. Similar phylogenetic analyses were performed for the
737 individual enzymes (see Extended Data Fig. 6). The taxonomic class for each organism was
738 retrieved from the NCBI taxonomy database using the R package taxize⁵⁴. Phylogenetic trees
739 were visualized in R using the packages ggtree⁵⁵, ape⁵⁶, treeio⁵⁷, and ggplot2⁵⁸.

740

741 **Phylogenetic analyses of ceramide synthesis genes**

742 To get a representative set of sequences from across the eukaryotic domain, we used BLASTP on
743 the NCBI server to find the top 500 eukaryotic hits for CerS from humans (CerS1, Accession
744 P27544.1), *Arabidopsis thaliana* (Lag1P, Accession NP_001184985), and *Saccharomyces*
745 *cerevisiae* (Lag1P, Accession AAA21579.1). The results were cleaned to remove duplicate hits;
746 in order to compare roughly the same number of proteins in each group, 250 hits were chosen at
747 random using the Linux “shuf” command. The same protocol was used for the following Spt and
748 KDSR queries: human (Accessions NP_006406.1 and NP_002026.1), *A. thaliana* (Accessions
749 NP_190447.1 and NP_187257), and *S. cerevisiae* (Accessions CAA56805.1 and P38342). The
750 yeast CerS and KDSR proteins were then used to find the closest homologues in bacteria using
751 BLASTP. Short-chain dehydrogenases similar to yeast KDSR were identified; by contrast, yeast
752 CerS had a single partial match (45% query coverage, E-value=4.0) in *Orenia metallireducens*.
753 *C. crescentus* CerR was used as a query to find the closest eukaryotic homologues, which
754 identified NDUF9A proteins. A reverse-BLAST identified CCNA_03718 as the closest *C.*

755 *crenscentus* NDUF9A homologue, which was then used to identify other bacterial NDUF9A
756 homologues. To trace the lineage of bCerS, we used the following protein queries to identify
757 eukaryotic Gcn5 proteins: human (Accession AAC39769.1) and *S. cerevisiae* (Accession
758 NP_011768.1). We identified bacterial GNAT proteins using *C. crenscentus* bCerS as a BLASTP
759 query to search the entire NCBI bacterial database. The eukaryotic Spt proteins were compared
760 to the bacterial Spt proteins identified in Supplemental Data 1. Phylogenetic trees for the Spt,
761 CerR/KDSR/NDUF9A, and CerS/Gcn5/GNAT/bCerS proteins were prepared with MUSCLE
762 and RAxML and visualized with R as described above.

763

764 **Methods references**

- 765 46 Poindexter, J. S. Selection for nonbuoyant morphological mutants of *Caulobacter*
766 *crenscentus*. *J Bacteriol* **135**, 1141-1145 (1978).
- 767 47 Ferrieres, L. *et al.* Silent mischief: bacteriophage Mu insertions contaminate products of
768 *Escherichia coli* random mutagenesis performed using suicidal transposon delivery
769 plasmids mobilized by broad-host-range RP4 conjugative machinery. *J Bacteriol* **192**,
770 6418-6427 (2010).
- 771 48 Martinez-Garcia, E., Calles, B., Arevalo-Rodriguez, M. & de Lorenzo, V. pBAM1: an
772 all-synthetic genetic tool for analysis and construction of complex bacterial phenotypes.
773 *BMC Microbiol* **11**, 38 (2011).
- 774 49 Bligh, E. G. & Dyer, W. J. A rapid method of total lipid extraction and purification. *Can*
775 *J Biochem Physiol* **37**, 911-917 (1959).

776 50 Guan, Z., Katzianer, D., Zhu, J. & Goldfine, H. *Clostridium difficile* contains
777 plasmalogen species of phospholipids and glycolipids. *Biochim Biophys Acta* **1842**, 1353-
778 1359 (2014).

779 51 Edgar, R. C. MUSCLE: a multiple sequence alignment method with reduced time and
780 space complexity. *BMC Bioinformatics* **5**, 113 (2004).

781 52 Stamatakis, A. RAxML version 8: a tool for phylogenetic analysis and post-analysis of
782 large phylogenies. *Bioinformatics* **30**, 1312-1313 (2014).

783 53 Miller, M. A., Pfeiffer, W. & Schwartz, T. Creating the CIPRES Science Gateway for
784 inference of large phylogenetic trees. *2010 Gateway Computing Environments Workshop*
785 *(GCE)*, 1-8 (2010).

786 54 Chamberlain, S. A. & Szocs, E. taxize: taxonomic search and retrieval in R. *F1000Res* **2**,
787 191 (2013).

788 55 Yu, G. Using ggtree to visualize data on tree-like structures. *Curr Protoc Bioinformatics*
789 **69**, e96 (2020).

790 56 Paradis, E. & Schliep, K. ape 5.0: an environment for modern phylogenetics and
791 evolutionary analyses in R. *Bioinformatics* **35**, 526-528 (2019).

792 57 Wang, L. G. *et al.* Treeio: An R Package for phylogenetic tree input and output with
793 richly annotated and associated data. *Mol Biol Evol* **37**, 599-603 (2020).

794 58 Wickham, H. *ggplot2: Elegant Graphics for Data Analysis*. (Springer-Verlag New York,
795 2016).

Figure 1

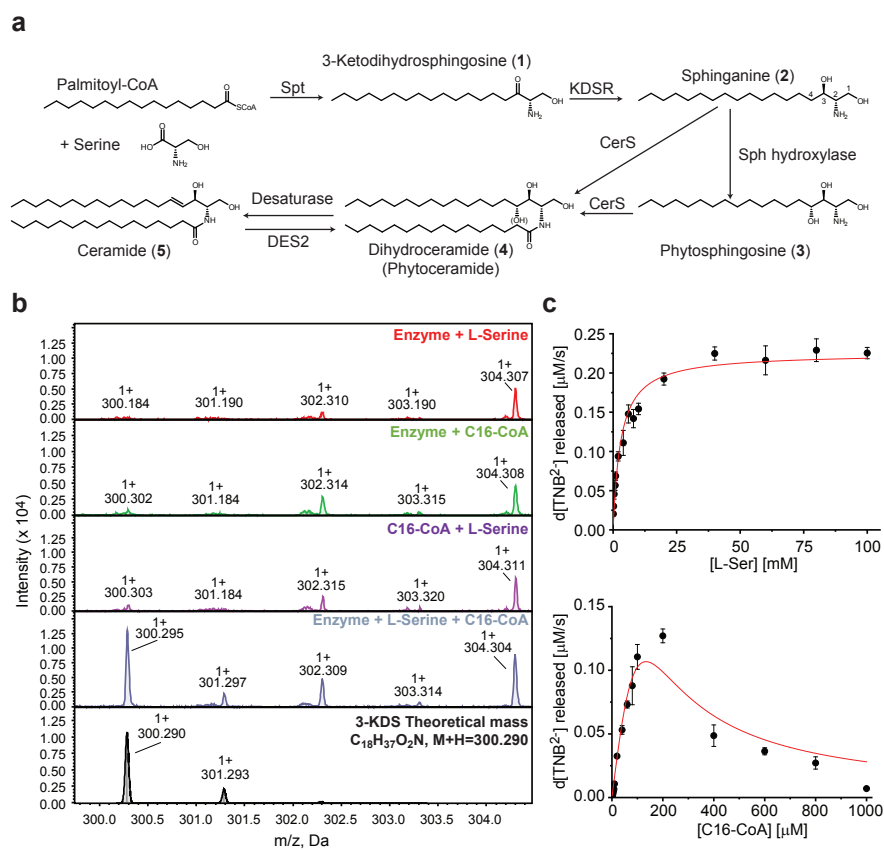


Figure 2

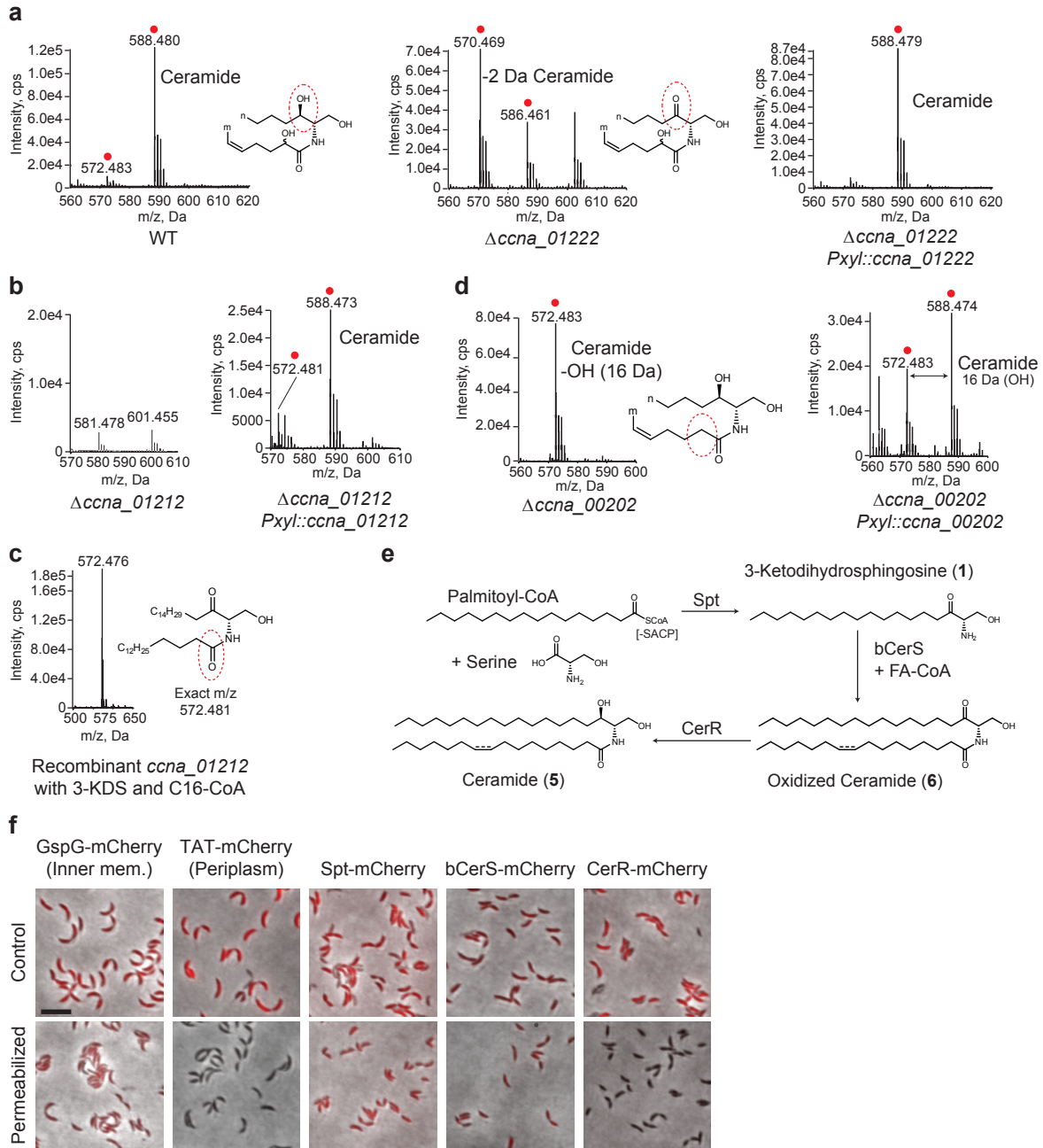


Figure 3

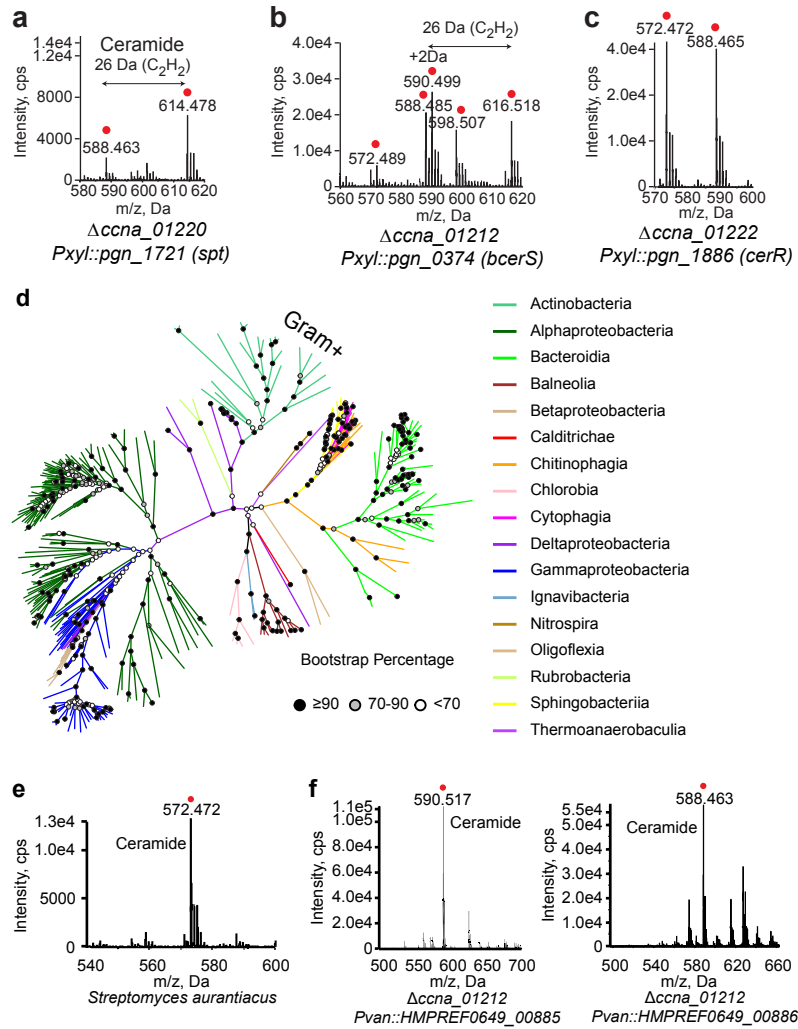
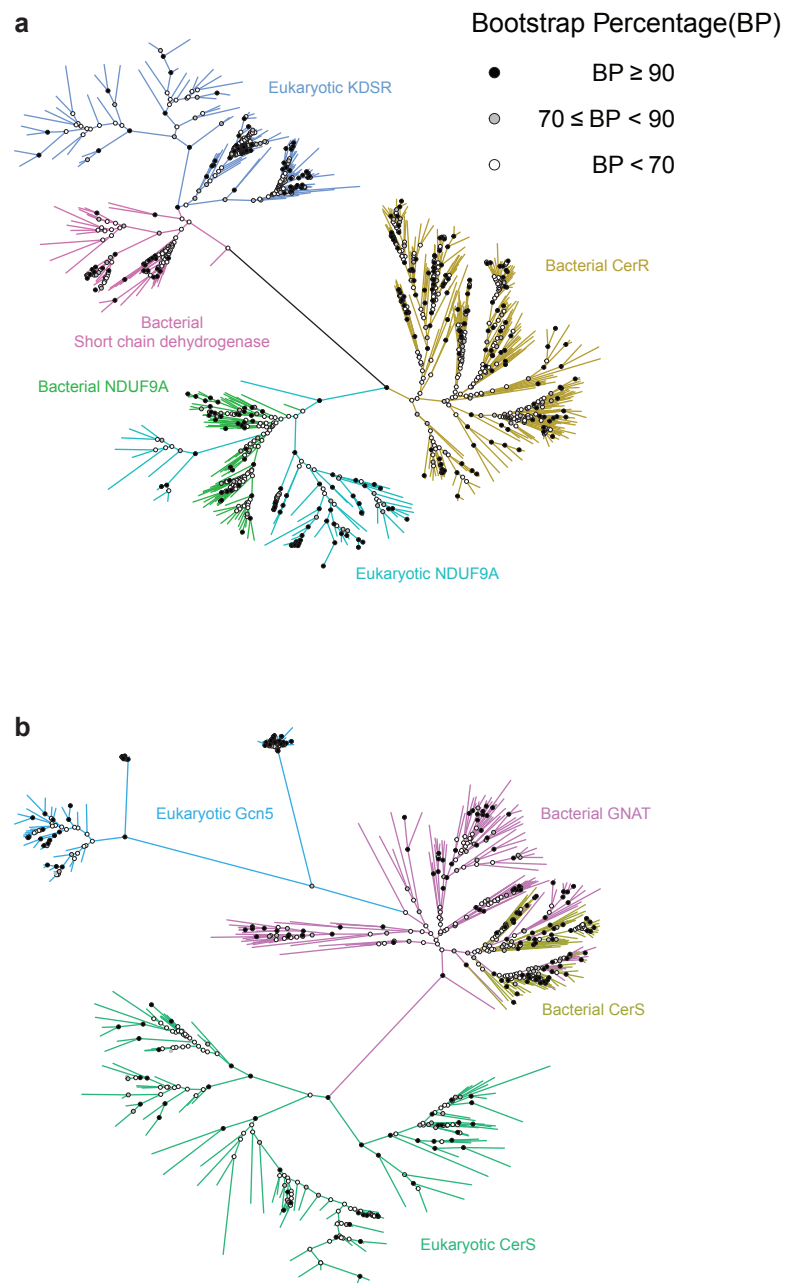
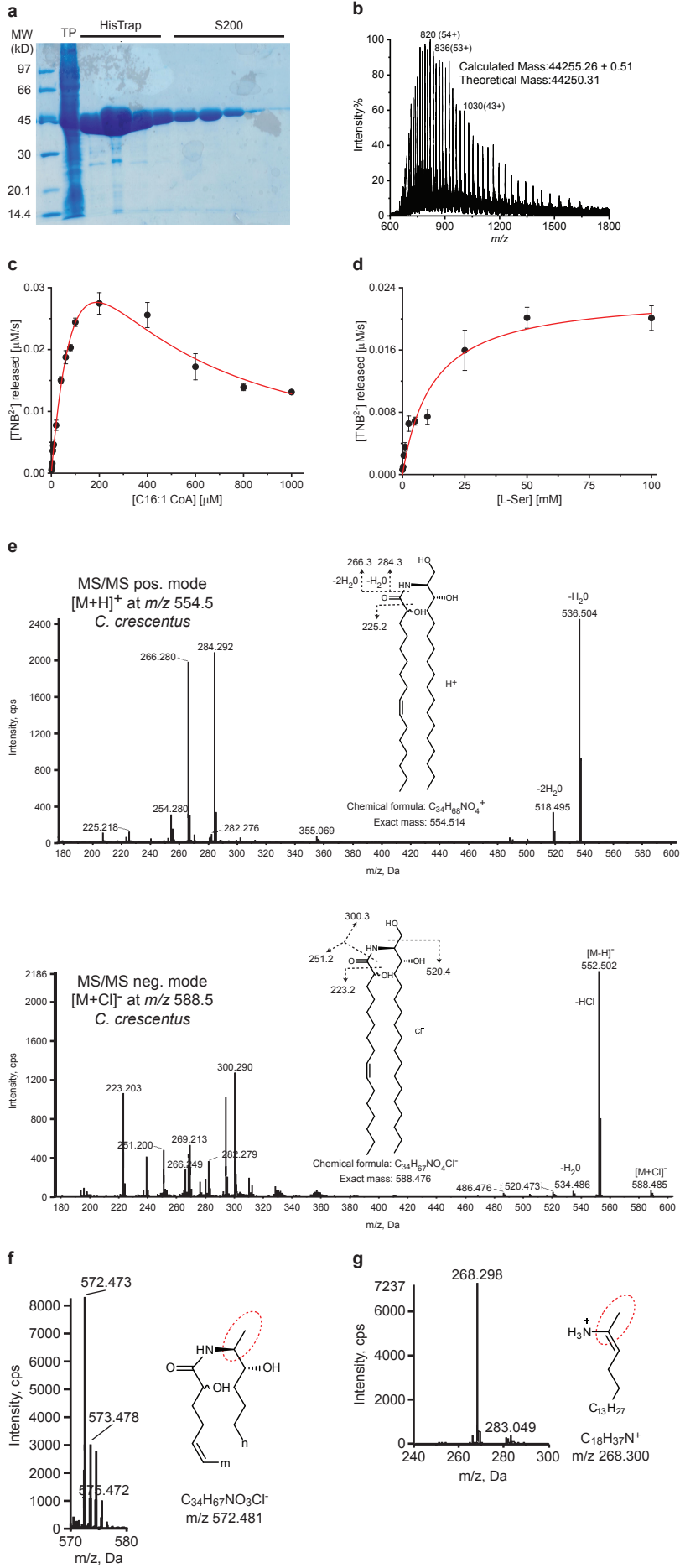


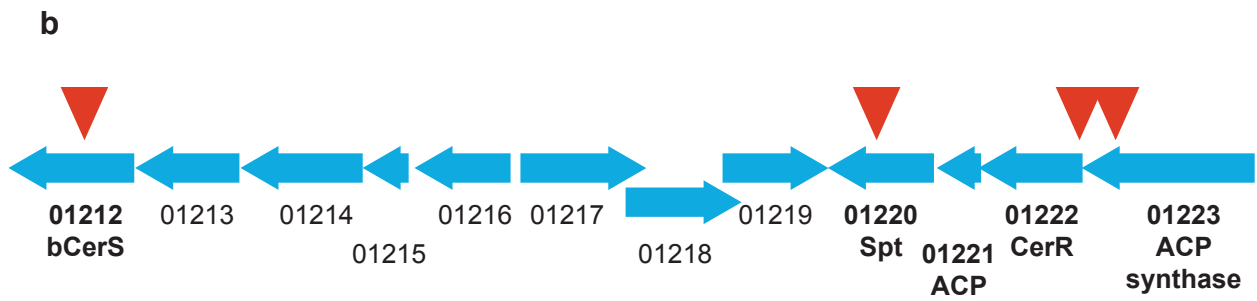
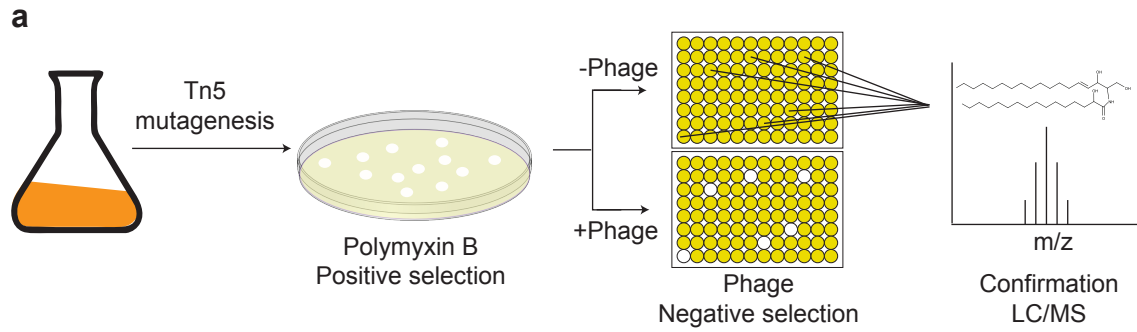
Figure 4



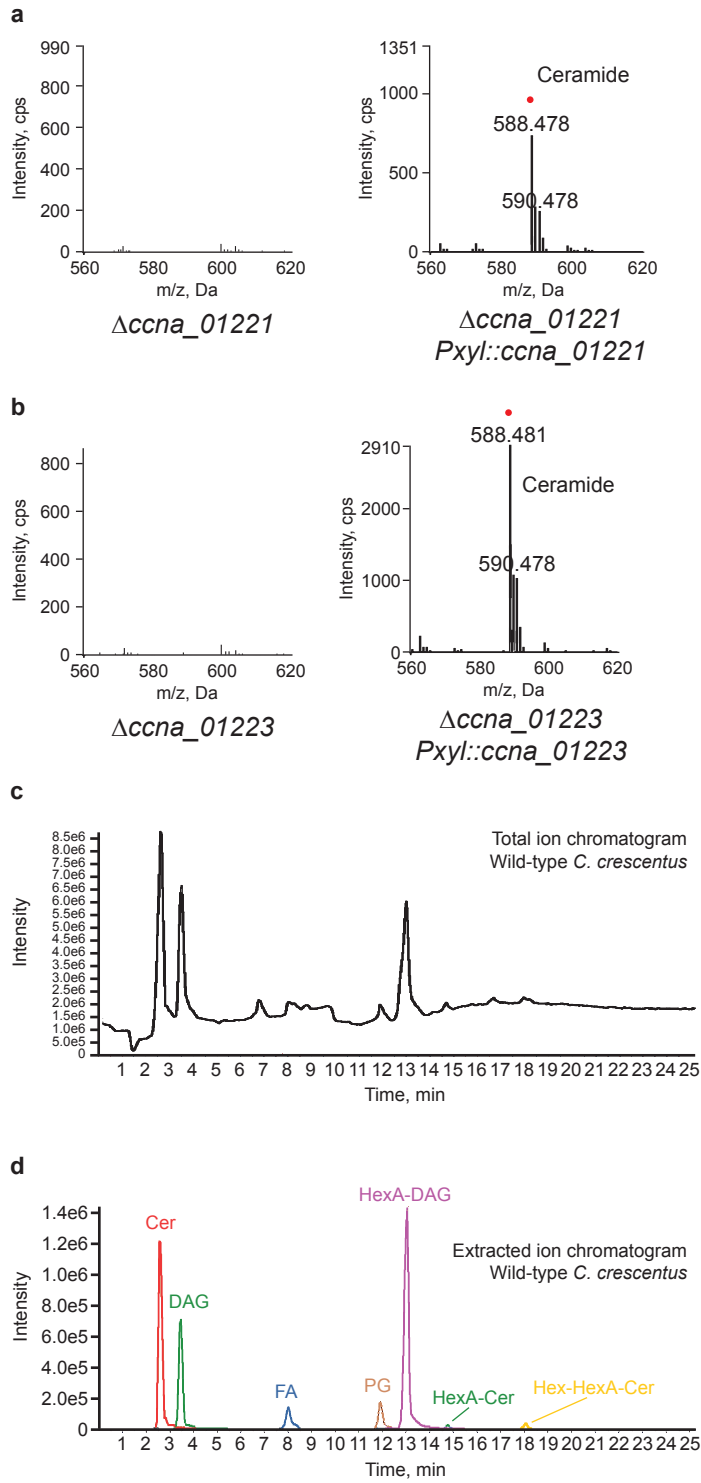
Extended Data Figure 1



Extended Data Figure 2

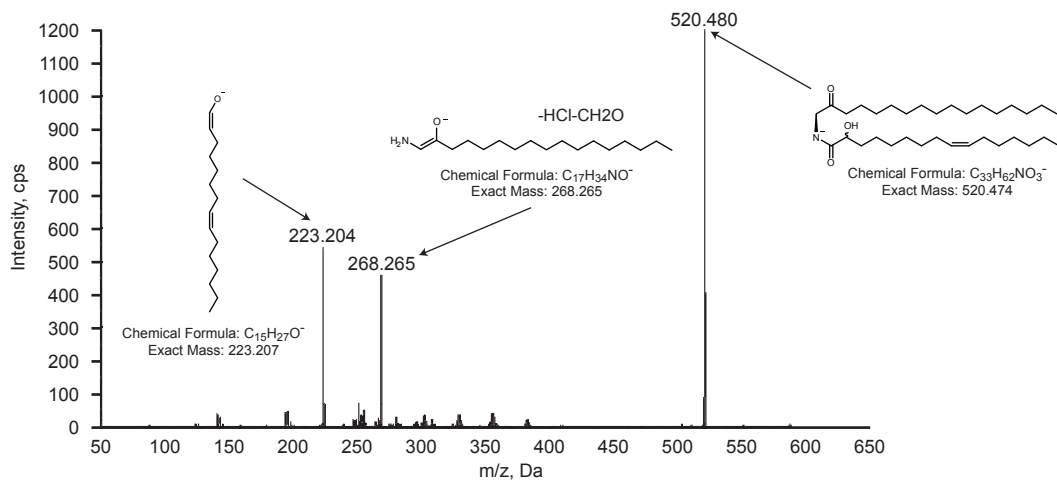
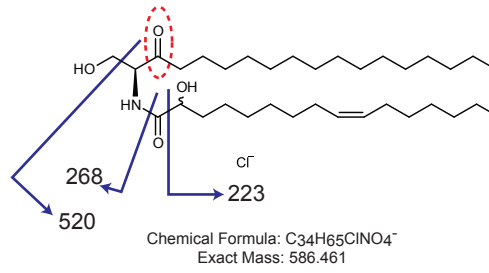


Extended Data Figure 3

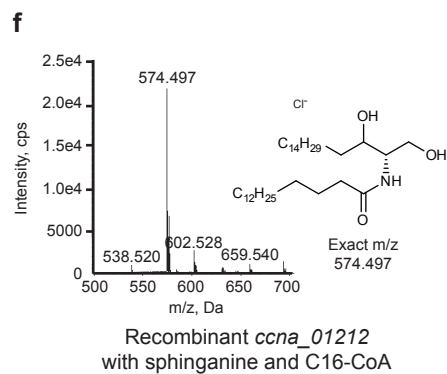
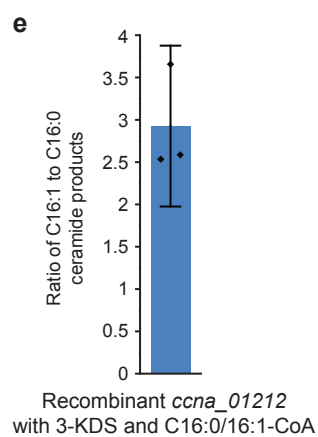
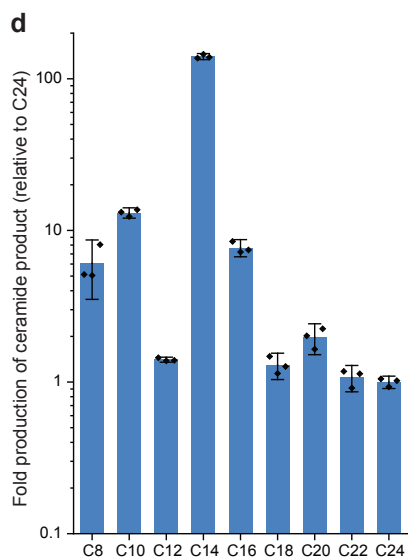
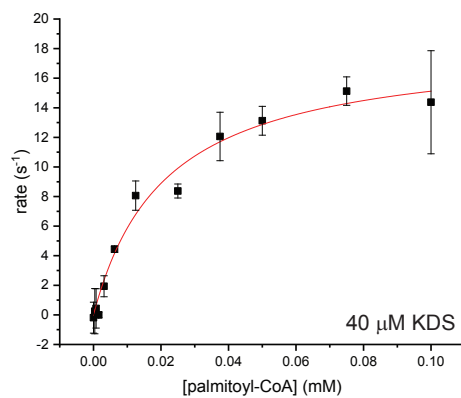
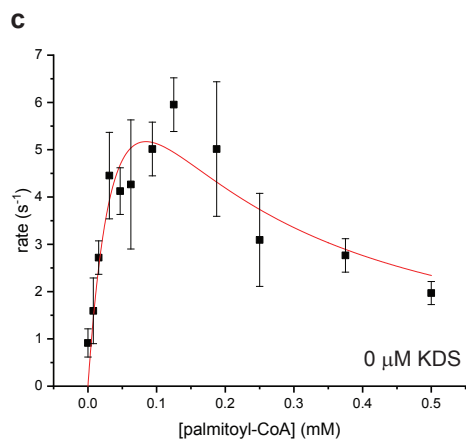
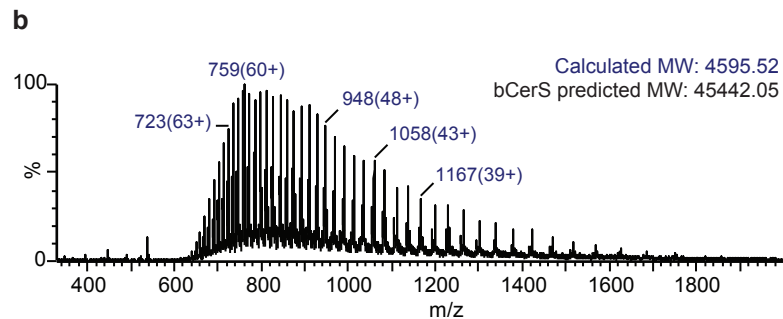
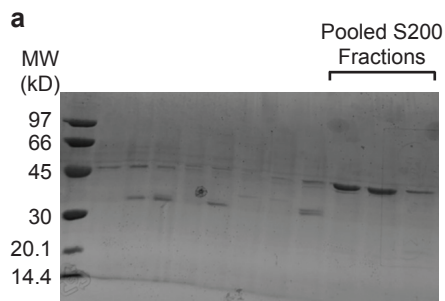


Extended Data Figure 4

MS/MS m/z 586.4
[ceramide-2Da+Cl⁻]

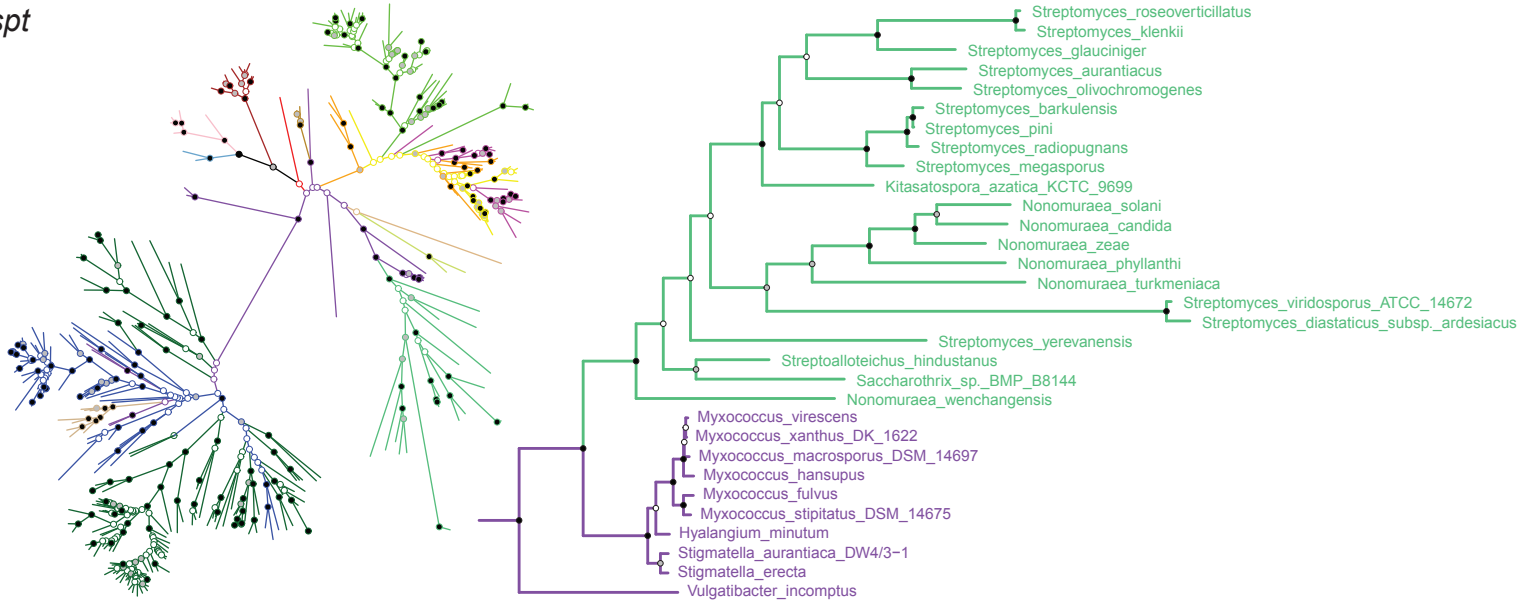


Extended Data Figure 5

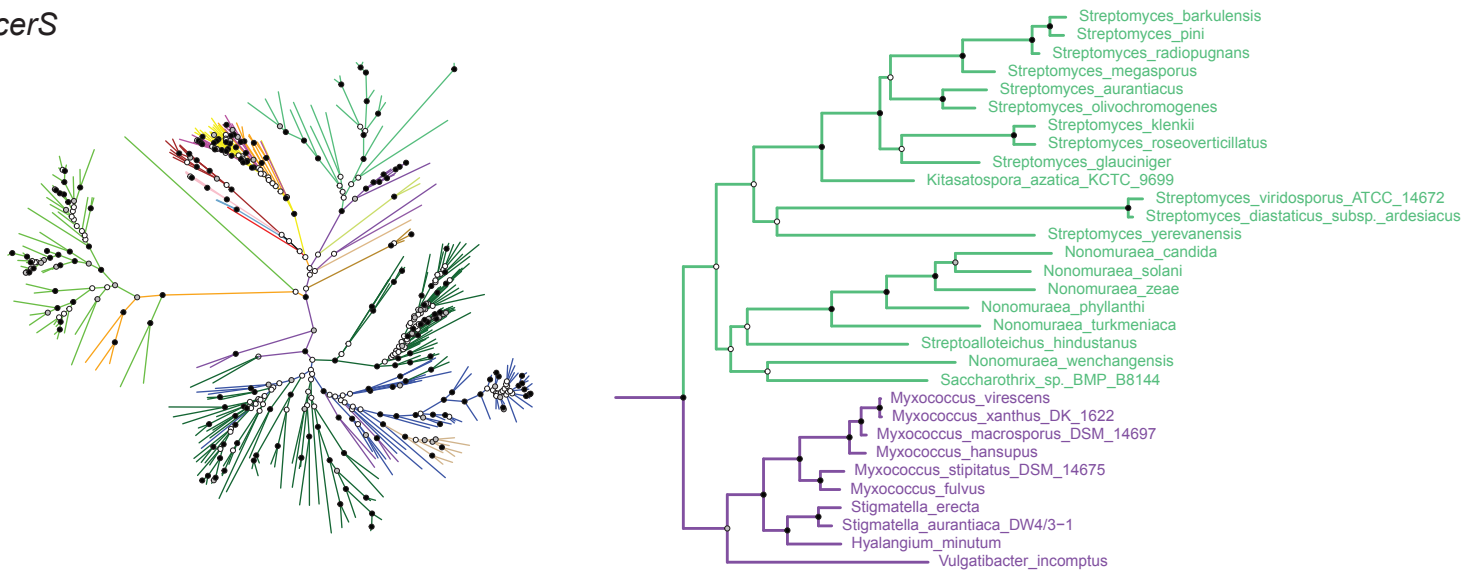


Extended Data Figure 6

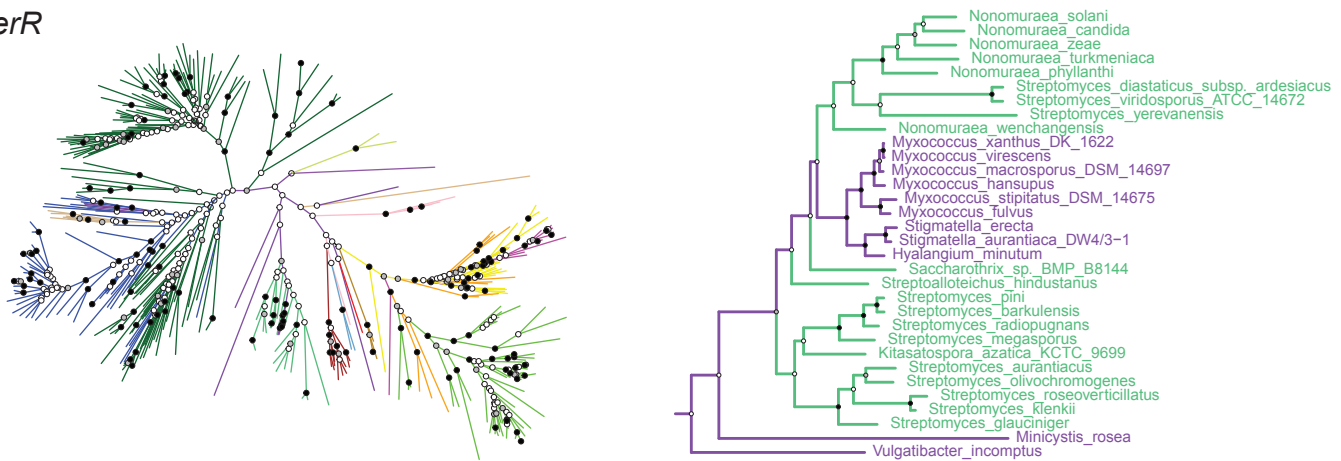
spt



bcrS



cerR



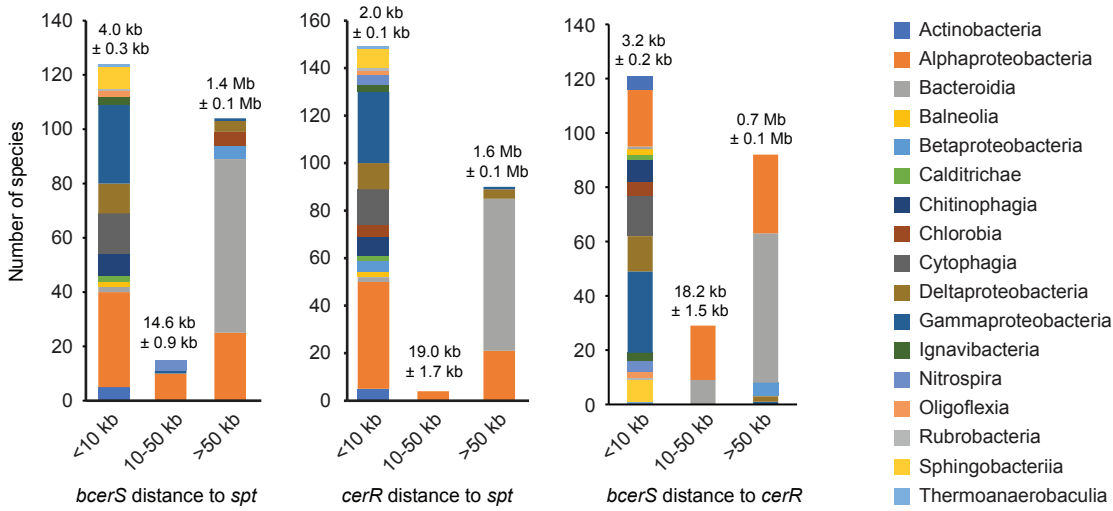
Bootstrap Percentage(BP)

- BP ≥ 90
- 70 ≤ BP < 90
- BP < 70

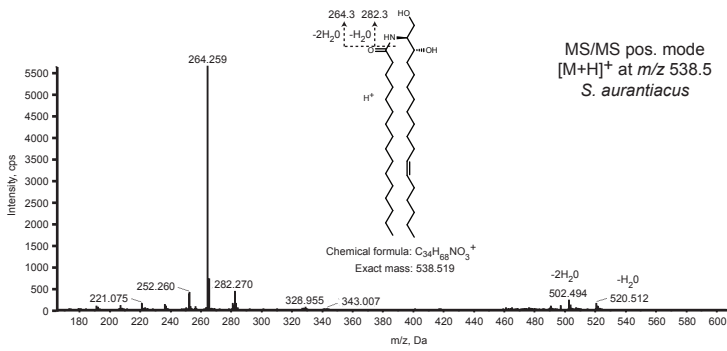
- Actinobacteria
- Alphaproteobacteria
- Bacteroidia
- Balneolia
- Betaproteobacteria
- Calditrichae
- Chitinophagia
- Chlorobia
- Cytophagia
- Deltaproteobacteria
- Gammaproteobacteria
- Ignavibacteria
- Nitrospira
- Oligoflexia
- Rubrobacteria
- Sphingobacteriia
- Thermoanaerobaculia

Extended Data Figure 7

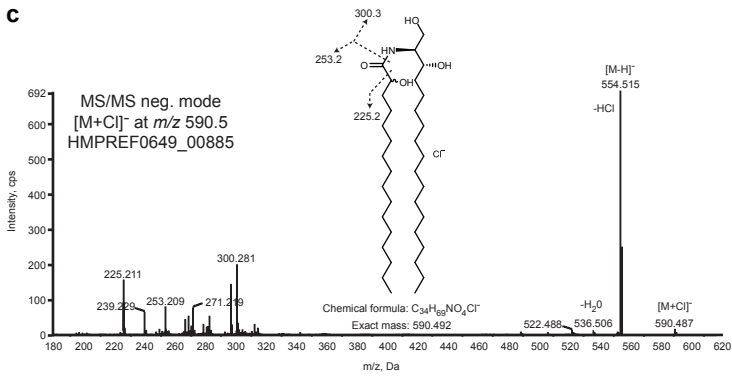
a



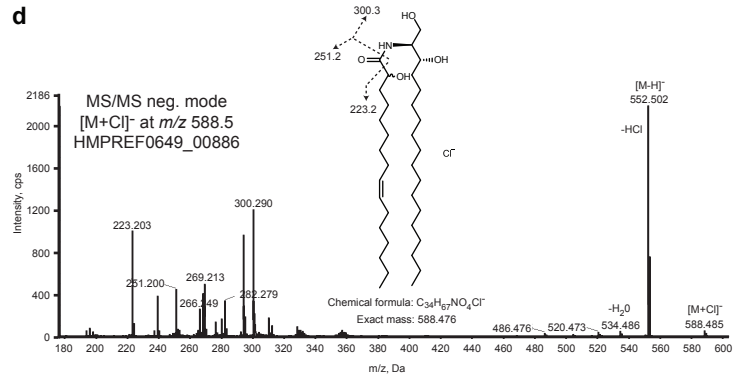
b



c



d



Extended Data Figure 8

Serine palmitoyltransferase alignment

Saccharomyces cerevisiae	1	-----MAHIPEVLP-KSI
Arabidopsis thaliana	1	-----
Homo sapiens	1	-MRPEPGGCCRRVRAN--GCVANGEVRNGYVRSSAAAAAAGQIHVVHTQNGGLYKRP--FNEAF
Caulobacter crescentus	1	-----
Porphyromonas gingivalis	1	-----
Bacteroides thetaiotaomicron	1	-----
Saccharomyces cerevisiae	13	PIPAFIVTSSYLWYFNLVLTQIPGGQFIVS-YIKKSHHDDPYRTTVEIGLIVGIYYLSKPQQKSL
Arabidopsis thaliana	1	-----
Homo sapiens	64	EETPMLVAVLTVYVGYGLTLFGYL--RDFLRVWRIEKCHHATE-REEQKDFVSLV-----
Caulobacter crescentus	1	-----MGLV-----
Porphyromonas gingivalis	1	-----ILQ-----
Bacteroides thetaiotaomicron	1	-----ILQ-----
Saccharomyces cerevisiae	82	QAQKPNLSPQE-IDAIIIDWE-----PEELVDPS--ATDEQSWRVAKTPVTMEMPIQNHITITRNNLQE
Arabidopsis thaliana	1	-----
Homo sapiens	116	-QDFENIYTRNLYMRIRLNWNRPICSVPGARVDIIEERQSHDYNWSFK-----YTGN
Caulobacter crescentus	5	-DKHLAIRD--AYKALIQVVG-----ANPFRVRFVAVHSP-----EGVV
Porphyromonas gingivalis	4	-ERLAKENT--PKEYMIRG-----LYPFREREIEGKQG--I-----EVDV
Bacteroides thetaiotaomicron	4	-EKLAKIDL--PQKFMAGQ-----VYPREREIEGKQG--I-----EVEM
Saccharomyces cerevisiae	143	KYTNVFNLASNNFLQLSATE-PVREVVKTTIKNYGVCACCPAGFYGNQDVHYTLEYPDLAQFEGTQISVLY
Arabidopsis thaliana	1	-----MLFLLSGTTAVHGELEECVAKFVGGKPLAVV
Homo sapiens	166	IIRGVINIGSYNYLGFARNTGSCQEAARVVEEYCAVCVSRQEIENLDKHEBLEELVARFLGVEVAAV
Caulobacter crescentus	41	DGRPTILIGTNNYLGTFDE-QATAASVKAQERGIGTTGSRIANGFESHVELEQELAKFYGRKHAVV
Porphyromonas gingivalis	38	GKKVIMFGSNAYTGLRGN-RVTEAGVEARRYGSGCAGSRFLNGTLDIHVQLEKELAEFVKKDBALCF
Bacteroides thetaiotaomicron	38	GGQVIMFGSNAYTGLRGN-RVTEAGIKARRYGSGCAGSRFLNGTLDIHVQLEKELAAVFGKDBALCF
Saccharomyces cerevisiae	212	GDFCAAPSVPFAFTRRGLIVADDQVSLPQNALQLSRSTVYFVHNDMNSLECLLNELTEQEKLEKLP
Arabidopsis thaliana	32	GMGLTNSLIISVILGAGGIIISPSLNHTSILNGARGSGATIRVFQHN-----ILKEHIEGQPRTHR
Homo sapiens	236	GMGFATNSMNPALVGNGLILSDELNHASIVLGARLSGATIRIFKHNNMQSLEKLLKDAIVYGPRTRR
Caulobacter crescentus	110	ITGQANLGVSTLVGRGDHILCADSHASTYDGSRLGHAENIRFVHNDPEDLAKRLRRLGDP-----
Porphyromonas gingivalis	107	FTGFTVNSGVIPCLGRNDYIICDDRHDASIVDGRRLSFSQQLKVKHNDMEDLEKQLQKCDP-----
Bacteroides thetaiotaomicron	107	STGFTVNSGVISCLTDRNDYIICDDRHDASIVDGRRLSFSQQLKVKHNDMADLEKQLQKCNP-----
Saccharomyces cerevisiae	282	AIPKFIIVTEGIIHNSGDIAPLPELTKLNKVKFRLFVDETFSIGVLGAVGRGLSEHNMRATALDITV
Arabidopsis thaliana	95	PWKALIVVEGIIISMEGIIICDLPEIVSICSEYKAYIYDEAHSIGALGKIGRGVCELLGVDIT-TEVDIMM
Homo sapiens	306	PWKALIVVEGIIISMEGIIIVRLPEVIALKKYKAYIYDEAHSIGALGPIGRGVVEVFGLEP-EVVDVMM
Caulobacter crescentus	172	APGELIVVEGIIISMEGIIICDVAPEIKETIAVKEEMGCVLLVDEAHSIVGLGAVGRGLAEAAAGVE--EVVDFIV
Porphyromonas gingivalis	169	NAV-KLIIVDSVFSMEGDIANLPEIVRLKKKYDAILLVDEAHGIVGVGKQGVCHHFGFLT--EVDLIM
Bacteroides thetaiotaomicron	169	DSV-KLIIVDGVFSMEGDIANLPEIVRLKHKYNAITIMVDEAHGIVGVGKQGRGVCHHFGFLT--HEVDLIM
Saccharomyces cerevisiae	352	GSMATALGSTGGFVLCDSVCLHQIRIGSNACFSACTPAYTTSVSKVLKMLDSN-----NLAQTLQK
Arabidopsis thaliana	164	GTFLKSLGSCGGIAGSKDLVQYLYQHYPAHYATSIPTAAQQVSAIKVIFGVDGNSRNGELKVAIRE
Homo sapiens	375	GTFLKSLGSCGGIAGSKKELIDYLRTHSHSAVYATSLSPVVEQIITSMCIMGQDGTSLGRCEVQQLAE
Caulobacter crescentus	240	GTFSKSLGATGGFCVSDHDDFVIRVICRPMYFASLPPVAASTTALERMIEQ-----PFLRDLNR
Porphyromonas gingivalis	236	GTFSKSLASITGGFIAGDSTINWIRHNARTYIFASLPPATAAAEALRTIRTE-----PERIDLWD
Bacteroides thetaiotaomicron	236	GTFSKSLASITGGFIADSSINWIRHNARTYIFASLPPATAAAEALHIQNE-----PERINALWE
Saccharomyces cerevisiae	416	LSRSIHDSFASDDSLRSYIVTSSPVSAVHLQLTPAYSRKFGYTCEQLFETMSALQKKSQTNKFIQY
Arabidopsis thaliana	234	NSNIFRAFLQKMG-EKVLVYSPILPLV-----LYNPAKIAARS
Homo sapiens	445	NIRYFRRLKEMG-FIIVYON-EDSPVPLV-----LYMPAKISAG
Caulobacter crescentus	304	NARLYDGLTAMG-FLTGPS--ASPIVAAT--EDQERAIAMW
Porphyromonas gingivalis	300	VTRVALKRFRFEG-EEGPH--ESPIEPLY--VDMERTFIVT
Bacteroides thetaiotaomicron	300	ATNVALRRFRFEG-EEGPH--ESPIEPLY--VDMERTFMVT
Saccharomyces cerevisiae	486	EEEEFLQSGIVHALINYVLTTRNTIVLQKQETLPIVPSIKICCNAAAMSPHELKNACESVKQSILA--CC
Arabidopsis thaliana	273	-----RECLRE-----NLAI---VVSFPEIPLLLARARICNSAHLFDLIKALQVLSRAGDLTGK
Homo sapiens	484	-----REMLKR-----NGV---VVSFPATPIIESRARFCLSAHTREILDALKEIDEVGDLLQK
Caulobacter crescentus	342	-----NGLLQA-----GVLI---NLALPPATPDSRPLIRASVSAHTDEQIDAVLKYTYGEIGALGVI
Porphyromonas gingivalis	338	-----LAFVTA-----GVFI---NVPVPPACAPQDTLVRVALMAHHTEQVDEAVMRKKCFQBLDIL
Bacteroides thetaiotaomicron	338	-----LAFVTE-----GVFI---NVPVPPACAPQDTLVRVALMAHHTEQVDSAVAEKLVKFAK----
Saccharomyces cerevisiae	554	QESN-----
Arabidopsis thaliana	328	YFTAAPKKQ---EEKNG-----NTSKFKLRI-----
Homo sapiens	539	YSRHLVLP---LDRPFDETTYEETD-----
Caulobacter crescentus	397	EPLKARA-----
Porphyromonas gingivalis	393	-----
Bacteroides thetaiotaomicron	-----	-----

Extended Data Figure 9

a

Bacterial CerR

Porphyromonas gingivalis	1	---VGNKRVLLTGATGFFGGYLVLEAARRQYVWAAVVRPHSDRSRLTDSRIRFLEIDYRD
Bacteroides thetaiotaomicron	1	-----LLLTGAAGFIFGFSFVVEAALKRKFVWAGLRPTSSKKYLKNRKIHFELELDFAH
Caulobacter crescentus	1	MATDARGVVAITGATGFFGRFLVRAIQDQWRPRVLRVRDVPVHPFWRDLVEVVTGDLGT
Sphingomonas paucimobilis	1	-----IIVAVTGTGTFVGRVVRVRSAGSGLSRALTRRAQPS-----RAGITWLAGALDK
Bacteriovorax stolpii	1	-----MKLLMTGASGFFGGHLLERLTKDGHVVFALVRNPKKLAIPAHERLQVVKGDLDQ
Myxococcus xanthus	1	-----LRFLITGTTGFFIGQRLARRIVERGDTTLVVRASSRRGPLEGLGARVFWADLIT
consensus	1*.....*
Porphyromonas gingivalis	58	PS--DIAR--LADKIAPEGESAWHLVIHNAGITKARITSLREINAEQOTRFILGLOAKH
Bacteroides thetaiotaomicron	53	PN--ELRAQ--SGHKGTYNK--FYIILHCAGITKCPKNTEDYVNYLQTYFYITLTKALNM
Caulobacter crescentus	61	FR--ALDRLAK-----GAVFVHVAGITKARTLEGFNRVNODGARAAAARAAA--
Sphingomonas paucimobilis	50	PD--SLATLVE-----GADAVIHLIAGVNAPIRAGEVAGNIDGTRATVAAKAA--
Bacteriovorax stolpii	55	DNLSWVETLPA-----DLNTCVHTAGIVHAYRTDEYRVNTEGTRNLVNNKPKKY-
Myxococcus xanthus	55	GA--GLAEAVR-----DVDVCHLHAGITKSRPEGIEGNAKGTNRRLVMAALP-
consensus	61 * *
Porphyromonas gingivalis	115	SPERFVLLSSMGSYGAP-PDDCQPLSSSSVFKPTIAYGSKLAEQYVRFVFTV--IIFYTI
Bacteroides thetaiotaomicron	109	VPKQFIYLSILSVFGVREKDYSPIEAGVVEPNVAYGLSKLKAELYQSIPG--FYFYVI
Caulobacter crescentus	108	G-ARFILLSSLAAREPS-----LSNYLASKRAGEDAVRAADP--SALI
Sphingomonas paucimobilis	97	GIKRFVHVSLSAREPA-----ISTYGWSKROAEAVITDSL---DWTI
Bacteriovorax stolpii	105	TSLHFVLLSSLAAGPSAGT--EKRNNNDMLPVSIIYGRSKKQAEVLEKAPKTFDLAV
Myxococcus xanthus	103	HFRRLVYCSLLAAGPSTPE--RPREEDPEAPVSIYGRSKLGEAVRAFADRV--SIVL
consensus	121 * * *
Porphyromonas gingivalis	172	IQPTGVYGHDDYLLMAI----RSVDKGFDFSTESTPQTLTFIYAEELASAFIAAHPD
Bacteroides thetaiotaomicron	167	YRPTGVYGPREDYFLMA----KSIQHVDFSVGFRRQDITFYVVKDVAQFLGIEK-K
Caulobacter crescentus	148	VRPPATYGPDDTETLGFQLAARSPVLPVLSQ----TSRVAMIHVEDAAAKLMAFCRTPV
Sphingomonas paucimobilis	138	VRPSGIYGPDMEMRDVFRAAKMRI--ALMPP---EGKVSIVAVEDEFARLTTLVTTDG
Bacteriovorax stolpii	163	IRPPMVIIGPRDAAVLD--FKMVQSGVI--LIPGFGSKEKLYSFCVFDVNTLVKVIIEKK
Myxococcus xanthus	160	VRPHIYVGPDEHLLPSSLPMALGLA--KSGFG--PKYSSLIHVDLCTALLAAARGP
consensus	181	..*.....*.....*
Porphyromonas gingivalis	228	A-----AGQKIVVSD--GNEYTDIEFGRMIOHLLGRKNVCHLRIFLPLVVKATCYGQKW
Bacteroides thetaiotaomicron	222	V-----TRRAYFLTD--GKYNSRVFSDLIQKELGNPFVIHVCPPLIVIKVLSLAEFI
Caulobacter crescentus	204	-----L-GLVELSDVRRDGYTTEIMRGAHVGA-KPRLRLPDPGILTAGALVDAW
Sphingomonas paucimobilis	192	-----PRAVLEVD--GQALTHAELANGICAAVQO-RVMTLHLP-KGLLQGAKIDRA
Bacteriovorax stolpii	221	-----TTVYSSH--PQVVTNEIILEIKKQIKKNWLIYLPMPLEFLVKLTIILDFI
Myxococcus xanthus	217	TVSKEDPARGVAVSD--GVEHSWEDVCTAMAGALGKGRPAVLPVFPQTVSYVGLGSEAV
consensus	241 *
Porphyromonas gingivalis	280	ADISGTLPLNLDKYAIIAQRNWRDSSP-IRALGFSRNVNLEQGLAETIRVARTTQGR
Bacteroides thetaiotaomicron	274	ATRSCKSSTLNSDKYIIMKQRNWCDDITPAINEICVAPENDLEKGRVETIDWYNEG---
Caulobacter crescentus	255	SSLTNTPTVFGLGKARELLHTDWTSSAPM--AEVPSKGLIDGFTHTVDWYRAAGWLP
Sphingomonas paucimobilis	241	--LRNGAKLTPDVGYLCHPDWTADEPAKRPDPALVEPAIALSKGLADTARNYRANGLL-
Bacteriovorax stolpii	271	YKFFPHPLRLTPDKYIEFAATNWTCDGAKTEKELGOVYNDERTITVTLIDYKSRNWI-
Myxococcus xanthus	275	ARLRCTVPLINLDKVEEMRCPAWTCTSTERANRELGLFETIPLAQLAGLTLAAYREAGGR-
consensus	301 * *
Porphyromonas gingivalis	339	R----
Bacteroides thetaiotaomicron	-----	
Caulobacter crescentus	313	KNIVA
Sphingomonas paucimobilis	-----	
Bacteriovorax stolpii	-----	
Myxococcus xanthus	-----	
consensus	361	

b

Eukaryotic and bacterial reductase alignment

human KDSR	1	MLLLAAAFVAVFVLLLYMVSPLISPKPILALPCAHVV--VTGGS SGIGVCLAE CYKQCAFITLVARNEDKI
C. crescentus CerR	1	-----MATDARGVVAITGATGFFGRFLVRAIQDQWRPRVLRVRDVPVHPFWRDLVEVVTGDLGT
consensus	1 * * *
human KDSR	70	LQAKKEIEMHSINDKQVVLCSVDVSQDYNQVENVIKQAQEKLGPMMLVNCAGAVSGKFEDLEVSTEE
C. crescentus CerR	43	HPFWRDIEVEVVTGDI--LGTGPRAL--KGAEVFIHVAGIKARTL-----EGEN
consensus	71	. . . * * *
human KDSR	140	RLMSINYLGSVYPSRAVITTMKEERV-GRIVFVSSQALQLGLFGFIAYSASKFAIRG---LAFALQVEMK
C. crescentus CerR	91	R---VNQDCARAA-----AEAARAACARELLVSSLAARE--PSLSNYAASKRAGEDAVRAADPSALIVR
consensus	141	* . * . * . * . * . * . * . * . * . * . * . * . * . * . * . * . * . *
human KDSR	206	FYNVYITVAYFPDTPGFAENRTRKPETRLI-----SETTSVCPEQVAKQIVKDAIQG
C. crescentus CerR	150	PPATY---GGDTETLGLFQLAARSEVLPVLSQTSRVAMIHVEDAAAKLVAFCTPVLGL-----
consensus	211	* . * . * . * . * . * . * . * . * . * . * . * . * . * . * . * . * . *
human KDSR	262	NFNSSIGSDGYMLSAITCGMAPVTSITEGLQQVTMGFR-----TIAIFYLGSDFSIVRRC
C. crescentus CerR	207	VELSDVRRDGYTWEEMRGAHVVMGAKPRIRPDPGLTAGALVDWSSSLTNPSPVFLGKARELLHTD
consensus	281	* . * . * . * . * . * . * . * . * . * . * . * . * . * . * . * . * . *
human KDSR	319	MMQREKSENAEKTA-----
C. crescentus CerR	277	WTSSAPMAIGVPSKFLIDGFTHTVDWYRAAGWLPKNIVA
consensus	351	. . * .

Extended Data Figure 10

a

Bacterial bCerS

Porphyromonas gingivalis	1	-----MAVEIREVLDKAEELKFFVQFNIDLYRNNYHVPGLIDEMMTLDRK
Bacteroides thetaiotaomicron	1	-----MAITIKKVKSTKRELKFFIRFNRYMYKGNPYSPVLDYDMLNFTFK
Caulobacter crescentus	1	-----MPFDSTNADLSVIVPKTPEALKRFIALPARLNAKDPNWTPLFMERTDALTF
Sphingomonas paucimobilis	1	-----ISIRPVATKRFRKTFVDFPEGLYADDPHWVPPKCEALGLITP
Bacteriovorax stolpii	1	-----MSKIFIREIELSNKKLNAFIDLPELETYKNDPHWVPLIKMALKDLNLP
Myxococcus xanthus	1	MALHAEPTHASSMPSDVQITPVRGEARMQFIRLPMALYRSDPHWVPPLEMRDFLDP
Streptomyces aurantiacus	1	-----HGRCAMTVTVTPEVGRATTAFFIRLPMAYYRDDLWVAPLEREQRAFLDP
consensus	1 * * *
Porphyromonas gingivalis	46	DRNPAEFCEAIYFLAYREGRIVGRIAGMINHR-----ANETWNQNNARFGEVDFINDNE
Bacteroides thetaiotaomicron	46	KNNAEFCEADYFLAYRDDKIVGRVAAITNNR-----ANEKWECKNVRFGWIDFIDDE
Caulobacter crescentus	53	KTNPFEDHAEVQLFLATRGGFDVGRISAQIDQLTPQPT---EGRLDGHFGMTAAEDDPA
Sphingomonas paucimobilis	44	EKNGWYSHAKAQLFLAENGRVVGRI SAHLDTLALAMDASKGFGPGTGFVGLMDAV-SE
Bacteriovorax stolpii	49	KHPFYKTADYKANLAYNDKVVVGRIMATHNHT-----YNKHENNSVGHFCFESIEDLE
Myxococcus xanthus	61	KKNPFEEYGELELFLARRGPDVVGRIAAIRNPR-----HMEIHGTKEGFFGLFECVNDAG
Streptomyces aurantiacus	51	HRNPFHTVGTVRLFLARRSGTIVIGRIAAIVDPR-----YQERHDLKCGQGFGLFECVDDTE
consensus	61 ** ** * *
Porphyromonas gingivalis	101	VVDALFHAVSEWARSKGMMDLQGGPFGTDMDHENGLIEGFDQLGTMATIYNAYYYPKQIE
Bacteroides thetaiotaomicron	101	VSSALIKTVEVWGERGMTHITGPIGTFDFDAEGMLIEGFDQLSTMATIYNHPYYPVHNE
Caulobacter crescentus	109	VENVLFRAAEVWLRARGRTHAVGPFNLSINEEVGLLVWGFDPPEMVLMGHDFVYAGPRVE
Sphingomonas paucimobilis	103	VERALLAKAEGWLRQCMTRAVGPPVQSIIWEEPGLLVQGFQDPTIMMGHARPEYQGWLE
Bacteriovorax stolpii	103	VAQGLVNVAAEFLKKGITSMVQGPVSNPGTNYECGLLDKYDAAEQIMMTYNPPYYETLFN
Myxococcus xanthus	116	VARTLLESAAATWRLRLGMDAMLGPNLSSNQDWGLLDGFDTPPVMMPHPNPPYYAALIE
Streptomyces aurantiacus	106	AAAALFNAAADWLGEQITRILGPISTINHECGVLDVGFDRPPTMLMHPNPAAYYPQLFT
consensus	121	. * * ** * * *
Porphyromonas gingivalis	161	RUGFIKDDQWKEYKIFV--PTEIPEKHRRRISEIVRQKYGLKTLKFRTRK-EVMPYAHRTF
Bacteroides thetaiotaomicron	161	RUGFEKDADWVEYKIYI--PDAIPEKHKRRISELIQRYNLRKIKYTSGRVIAKDYGQEIF
Caulobacter crescentus	169	EQGAKAQAQLFAYKADE--TGDIPETAQRVKGGLPS-GVVLRQIDM--SRVDQEVQTEIT
Sphingomonas paucimobilis	163	AVGTTTIKQLEFYELDI--TQEFFPLVQRIIKSGEKNERIRVREVNK--AKPEEEAAITL
Bacteriovorax stolpii	163	EMGFFKAMDLLAYNISP--DIKIPQITVDIAATEKKSKVTVYRVDL--KMKKELEITF
Myxococcus xanthus	176	ACCLTKAKDLYAYELSS--SAQPEKVVRIAERKIRVVDGVRVFPVNM--KDLDAEVKRRIR
Streptomyces aurantiacus	166	DCGFTKAKDILLSRVPPADGEPVAVIRRAERALSAPVVRPVMNR--REDTDMAAAIR
consensus	181	. * * . *
Porphyromonas gingivalis	218	RITNKAYSQLYGFESELSAQIDYYVNIYIPVRLDFVTVIVREEDDEVIAHSTMPNLSR
Bacteroides thetaiotaomicron	219	ELMNEAYSPLNGYSPITQRQIYQVVMYLPITDLRNVTLIT--DADKLVCVGISMPLSAE
Caulobacter crescentus	224	EIINDAWSNDWGFTEPTTAETRQLKSLKQVIDQRLVWF---SEIDGEEAGVVVFLRNVNE
Sphingomonas paucimobilis	219	SIINDAWSNDWGFTEPTPEEIKDVGVKLPVFNLLIRI--AEIDGKPVAFMTLPLDINE
Bacteriovorax stolpii	219	EIYNSAWEANWGFVPMTKAEFDHTAKDLKATVDPTLIQY--AMVDGKEAGFIALPDLNQ
Myxococcus xanthus	232	EIYNSAWEKWGFVPTFAEFDHLAKELKTVVRPDLALM--AEVQGEPPVAFSLVTPDANQ
Streptomyces aurantiacus	224	EIYNDAWSNENASVPMTEPEFAHTIQKPMIRPELVQI--AEVHGEPVAFSLVLPDINQ
consensus	241	. . . * . * *
Porphyromonas gingivalis	278	ALRKAK-GSLWPFQFVHLLKAL---KGRPRVDFYLLGLVPEYQNKGVNA----LIFDNM
Bacteroides thetaiotaomicron	278	ALQKSH-GRLLPLGWFYLLKAL-FMKFRAKMLDILLVAVKPEYQNKGVNA----LLFSDI
Caulobacter crescentus	282	AADLK-GRLLPFGWAKLLWELK--VGVKSARPLMGVKKKETSQRGRMLPFWMKAS
Sphingomonas paucimobilis	277	AMPPLK-GSLLPFGWAKLLWELR--APKVRTMRVPLMGVVKELQSSRNASQALAFMMIEYT
Bacteriovorax stolpii	277	VETIIPSGRL---GPVALFKLLTAKSRINRARVIMMGVKKERKMGLET----LLYKNL
Myxococcus xanthus	290	ALFAAN-GRITTEGLPIGLVKKLALASFRINRRLIIGIKEGYRRRGLDA----ILLLDT
Streptomyces aurantiacus	282	ALFAAR-GRITTYGLPLGLLRVQHAASINRIRVVAAGVKKEHRVRGLAV----ALFTQA
consensus	301	. . . * . *
Porphyromonas gingivalis	330	IP-IFQKNGVEYAESNPELETNMAVQMQWNYFERK-HKTRRAEIKRL
Bacteroides thetaiotaomicron	332	IP-VYQKLGIFAESNPELELNGKVCAQWDYFETKQHKRRRAETKEI
Caulobacter crescentus	339	RD-VAMSLGNRYEISWLEANKATHTIAENVGTEHYKTYRYEKAL
Sphingomonas paucimobilis	334	RRASITKYGASRCEIGWLLDNQGRSIAETINSRVNKTYNVYARDL
Bacteriovorax stolpii	329	QVSQQNSRIKNVELSWLEETNVEVNNKPLIRMSPAYKRYRYEKAL
Myxococcus xanthus	345	LRTAKR-LGVGGEISWLEDNHLVNPAAIESMGAQFSKTYRYTRAL
Streptomyces aurantiacus	337	QRTAFR-LGVTEECSWLEDNDRANRSTKALGTEFRTHRYERA-
consensus	361 * * . *

b

Eukaryotic CerS Lag1P conserved domain

<i>S. cerevisiae</i>	222	RKDYKELVFFHHIVTLLLIWSSYVFHETKMGLATYITMDVSDFFLSLTKTLNY
<i>A. thaliana</i>	128	RSDFGVSMGHHIATLLILVLSYVCSHSRVGSSVLLALHDASDVLELVGKMSKY
<i>H. sapiens</i>	150	RKDSVVMLLHHVVTLLLIWSSYAFRYHNVGILVLFHLDISDVQLEFTKLNLY
<i>M. musculus</i>	150	RKDSVVMLVHHVVTLLLIWSSYAFRYHNVGLLVFLHDVSDVQLEFTKLNLY
<i>D. rerio</i>	154	RKDSLVMVHHFITLALITFSYAFRYHNIIGILVLFHLDINDVQLEFTKLNLY
consensus	241	* * * * * * *

